

Document downloaded from:

<http://hdl.handle.net/10251/182941>

This paper must be cited as:

Morelli, L.; Paulisic, S.; Qin, W.; Iglesias-Sanchez; Roig-Villanova, I.; Florez-Sarasa, I.; Rodriguez Concepción, M.... (2021). Light signals generated by vegetation shade facilitate acclimation to low light in shade-avoider plants. *Plant Physiology (Online)*. 186(4):2137-2151. <https://doi.org/10.1093/plphys/kiab206>



The final publication is available at

<https://doi.org/10.1093/plphys/kiab206>

Copyright American Society of Plant Physiologists

Additional Information

1 **Short title:** Shade-avoider plant acclimation to low light

2 **Corresponding author:** Jaime F. MARTINEZ-GARCIA (jaume.martinez@ibmcp.upv.es)

3

4 **Light signals generated by vegetation shade facilitate acclimation to low light in**
5 **shade-avoider plants**

6

7 Luca MORELLI^{1,2}, Sandi PAULIŠIĆ², Wenting QIN^{1,2}, Ariadna IGLESIAS-SANCHEZ², Irma
8 ROIG-VILLANOVA^{2,a}, Igor FLOREZ-SARASA², Manuel RODRIGUEZ-CONCEPCION^{1,2,*},
9 Jaime F. MARTINEZ-GARCIA^{1,2,3,*}

10

11 1, Institute for Plant Molecular and Cell Biology (IBMCP), CSIC-UPV, 46022 València, Spain.

12 2, Centre for Research in Agricultural Genomics (CRAG) CSIC-IRTA-UAB-UB, Campus UAB
13 Bellaterra, 08193 Barcelona, Spain.

14 3, Institució Catalana de Recerca i Estudis Avançats (ICREA), Passeig Lluís Companys 23, 08010
15 Barcelona, Spain.

16

17 a, current address, Barcelona School of Agricultural Engineering (ESAB), Universitat Politècnica
18 de Catalunya (UPC), Castelldefels, 08860 Barcelona, Spain.

19

20 *Correspondence to:

21 JFMG (jaume.martinez@ibmcp.upv.es)

22

23 **One-sentence summary:** Vegetation proximity light signals inform shade-avoider plants to adjust
24 their photosynthetic capacity in anticipation of eventual shading by nearby plants.

25

26 **Author contributions:**

27 MRC and JFMG conceived the original research plan, directed and coordinated the study. LM, IF-
28 S, AI-S and MR-C measured and analyzed photosynthetic parameters, respiration and pigment
29 levels; SP, IR-V and WQ performed all the other experiments. All authors analyzed their data and
30 discussed the results. MRC and JFM-G wrote the paper with revisions and contributions or/and
31 comments of all other authors.

32

33 **Funding information:** LM received a predoctoral fellowships from *La Caixa Foundation*
34 (INPhINIT fellowship LCF/BQ/IN18/11660004). WQ is a recipient of a predoctoral Chinese
35 Scholarship Council (CSC) fellowship. AI-S is supported by a predoctoral fellowship from
36 MICINN (PRE2018-083610). IF-S has received funding from the European Union’s Horizon 2020
37 research and innovation programme under the Marie Skłodowska-Curie grant agreement no.
38 753301. Our research is supported by grants from MICINN-FEDER (BIO2017-85316-R, and
39 BIO2017-84041-P) and AGAUR (2017-SGR1211, 2017-SGR710 and Xarba) to JFM-G and MRC.
40 We also acknowledge the support of the MINECO for the “Centro de Excelencia Severo Ochoa
41 2016-2019” award SEV-2015-0533 and by the CERCA Programme / Generalitat de Catalunya.

42 **ABSTRACT**

43 When growing in search for light, plants can experience continuous or occasional shading by other
44 plants. Plant proximity causes a decrease in the ratio of red to far-red light (low R:FR) due to the
45 preferential absorbance of red light and reflection of far-red light by photosynthetic tissues of
46 neighboring plants. This signal is often perceived before actual shading causes a reduction in
47 photosynthetically active radiation (low PAR). Here we investigated how several Brassicaceae
48 species from different habitats respond to low R:FR and low PAR in terms of elongation,
49 photosynthesis and photoacclimation. Shade-tolerant plants such as hairy bittercress (*Cardamine*
50 *hirsuta*) displayed a good adaptation to low PAR but a poor or null response to low R:FR exposure.
51 By contrast, shade-avoider species, such as Arabidopsis (*Arabidopsis thaliana*), showed a weak
52 photosynthetic performance under low PAR but they strongly elongated when exposed to low
53 R:FR. These responses could be genetically uncoupled. Most interestingly, exposure to low R:FR of
54 shade-avoider (but not shade-tolerant) plants improved their photoacclimation to low PAR by
55 triggering changes in photosynthesis-related gene expression, pigment accumulation and chloroplast
56 ultrastructure. These results indicate that low R:FR signaling unleashes molecular, metabolic and
57 developmental responses that allow shade-avoider plants (including most crops) to adjust their
58 photosynthetic capacity in anticipation of eventual shading by nearby plants.

59

60 **Key words:** chloroplasts, elongation, light, photoacclimation, photosynthesis, shade-avoider,
61 shade-tolerance.

62 INTRODUCTION

63 Light is essential for plants as a source of energy and environmental information. Shading by
 64 nearby individuals can reduce light quantity (i.e. photon supply) and hence compromise
 65 photosynthetic activity and growth, a problematic situation in intensive cropping systems. To deal
 66 with the outcomes of mutual shading, plants have developed response mechanisms based on the
 67 perception of light quality, i.e., spectral information (Casal, 2013; Martinez-Garcia *et al*, 2010). The
 68 preferential absorbance of red light (R) and reflection of far-red light (FR) by photosynthetic tissues
 69 results in a decreased ratio of R to FR (R:FR) when light is reflected from or filtered through green
 70 stems and leaves. The low R:FR is a very reliable light signal that announces the close presence of
 71 nearby plants that may compete for resources.

72 Plants growing in ecosystems where access to light is restricted (e.g., in forest understories)
 73 show a shade-tolerant habit by adapting their light capture and utilization systems to low light
 74 intensity conditions. By contrast, plants growing in open habitats are shade-avoiders (also referred
 75 to as shade-intolerant or sun-loving). In shade-avoider plant species, such as *Arabidopsis*
 76 (*Arabidopsis thaliana*) and most sun-loving crops, perception of the low R:FR signal by the
 77 phytochrome photoreceptors activates a signaling pathway that eventually triggers a set of
 78 responses known as the shade avoidance syndrome (SAS). The most prominent phenotype
 79 following exposure to low R:FR is elongation (e.g., of seedling hypocotyl, leaf petiole and stem
 80 internode tissues), intended to overgrow neighboring competitors and outcompete them in the
 81 access to light. If the neighboring individuals overgrow and eventually shade the plant, the
 82 consequent reduction in light quantity (i.e., in the amount of radiation available for photosynthesis)
 83 results in additional and stronger SAS responses such as reduced leaf size, attenuated defense
 84 mechanisms and early flowering (Roig-Villanova & Martinez-Garcia, 2016).

85 The most extensively studied SAS response by far is hypocotyl elongation in *A. thaliana*. In
 86 this species, low R:FR inactivates phytochrome B (phyB), releasing PHYTOCHROME
 87 INTERACTING FACTORS (PIFs) that can then regulate gene expression and promote elongation
 88 growth. This response is also repressed by negative SAS regulators such as ELONGATED
 89 HYPOCOTYL 5 (HY5), amongst many others (Cifuentes-Esquivel *et al*, 2013; Ciolfi *et al*, 2013).
 90 Biological activity of these transcription factors can be modulated by additional components of the
 91 SAS regulatory network such as LONG HYPOCOTYL IN FAR-RED 1 (HFR1, which binds PIFs
 92 to prevent their binding to target genes) and phytochrome A (phyA, which gets stabilized in shade
 93 and then promotes HY5 accumulation) (Ciolfi *et al*, 2013; Martinez-Garcia *et al*, 2014; Yang *et al*,
 94 2018). Both HFR1 and phyA hence act as additional SAS repressors that were recently found to be
 95 instrumental for the adaptation to shade. Indeed, the shade-tolerant hairy bittercress (*Cardamine*

96 *hirsuta*), a close relative of *A. thaliana*, does not elongate when exposed to low R:FR unless the
97 function of phyA or HFR1 is genetically lost in mutant plants (Hay *et al*, 2014; Molina-Contreras *et*
98 *al*, 2019; Paulisic *et al*, 2021).

99 Differences between shade-avoider and shade-tolerant species are not restricted to changes in
100 elongation after exposure to low R:FR. Photoacclimation (i.e., the ability of plants to adjust
101 photosynthesis to changes in the incident light with specific phenotypic changes) also diverges.
102 Variation of photoacclimation responses among species on day-to-week time scale has been
103 associated to two main strategies (Murchie & Horton, 1997; Ptushenko & Ptushenko, 2019). The
104 first one consists of an alteration of photosynthetic pigment content, which positively corresponds
105 with photosynthetic capacity. The second one involves changes in the photosynthetic machinery,
106 which appears to be more important in plant species from environments where temporal and spatial
107 variations in light irradiance are common, e.g., margins of woodlands. Combinations of these two
108 main strategies give rise to the observed diversity in photoacclimation. In the case of *A. thaliana*
109 and *C. hirsuta*, a differential response to low R:FR in terms of photosynthetic pigment
110 accumulation has been observed. Chlorophyll and carotenoid levels drop about 20 % in *A. thaliana*
111 plants grown under low R:FR conditions, whereas the decrease is attenuated in *C. hirsuta* plants
112 (Molina-Contreras *et al*, 2019). Whether photosynthetic capacity and/or chloroplast ultrastructure is
113 differentially impacted by low R:FR in these species remains unknown. In terms of light quantity,
114 the shade-avoider *A. thaliana* showed a lower capacity to acclimate to reduced photosynthetically
115 active radiation (low PAR) but a higher capacity to acclimate to intense light (high PAR) compared
116 to the shade-tolerant *C. hirsuta* (Molina-Contreras *et al*, 2019). A similar physiological behavior
117 has been described for shade-avoider and shade-tolerant species of the genus *Tradescantia* (Benkov
118 *et al*, 2019), a model to study the ecology of photosynthesis and the mechanisms of
119 photoacclimation in plants (Ptushenko & Ptushenko, 2019). The possible connections between low
120 R:FR signaling and photoacclimation responses in plants remain, however, virtually unknown. Here
121 we explored natural and engineered genetic diversity to investigate this connection using different
122 Brassicaceae species.

123

124

125 **RESULTS**

126 **Different Brassicaceae species present divergent photoacclimation responses**

127 We previously showed that, compared to sun-loving *A. thaliana* Col-0 (At), shade-tolerant *C.*
128 *hirsuta* Ox (Ch) exhibits a better ability to maintain photosynthesis after transfer to low PAR but a
129 stronger chlorophyll loss when light intensity increases (Molina-Contreras *et al*, 2019). To better

130 characterize the photoacclimation responses of these two Brassicaceae species, both At and Ch were
131 germinated and grown for 7 days under control conditions of a photosynthetic photon flux density
132 in the PAR region (PPFD) of 20-24 $\mu\text{mol m}^{-2} \text{s}^{-1}$ (W_{20}). Then they were transferred to either lower
133 PAR (W_4 , PPFD of 4 $\mu\text{mol m}^{-2} \text{s}^{-1}$) or higher PAR (W_{200} , PPFD of 200 $\mu\text{mol m}^{-2} \text{s}^{-1}$) for up to 7
134 more days (Fig. 1). Light curve analysis at day 3 after the transfer already showed clearly opposite
135 responses of At and Ch, i.e., a better photosynthetic activity of Ch compared to At when transferred
136 to W_4 and a better activity of At compared to Ch when transferred to W_{200} (Fig. 1A). Derived
137 parameters such as maximum electron transport rate (ETR_m) and photosynthetic rate in light-
138 limited region of the light curve (alpha) also illustrated that At performed better than Ch after
139 transfer to higher light (W_{200}) but worst after transfer to lower light (W_4) (Fig. 1B). Other
140 photosynthetic parameters such as maximum quantum efficiency of PSII (F_v/F_m) and light use
141 efficiency of PSII (ϕPSII) also showed differences between At and Ch at day 3 after transfer, but
142 these differences became clearer at longer times of exposure to either W_{200} or W_4 (Fig. 1C).
143 Specifically, F_v/F_m values were lower in Ch than in At after transfer to higher light, while the
144 opposite was observed when transferred to lower light. A similar trend was observed in the case of
145 ϕPSII (Fig. 1C). These results together indicate that Ch tolerates better the transfer to lower PAR
146 (consistent with Ch being more tolerant to shade), while an increase in light irradiance compromises
147 photosynthetic efficiency in Ch more than in shade-avoider At. Based on these results, we used
148 light curve analysis at day 3 or earlier to estimate photoacclimation to lower PAR and F_v/F_m
149 measurements at day 7 to estimate photoacclimation to higher PAR.

150 Besides At and Ch, the Brassicaceae family (mustards) includes many food crops (e.g.,
151 cauliflower, broccoli, radish, cabbage, kale, and similar green leafy vegetables) and a diversity of
152 wild species from forested and open habitats. As a first step to explore the possible connection
153 between low PAR and low R:FR responses, we analyzed photoacclimation and hypocotyl
154 elongation in six different Brassicaceae species or accessions, including At and Ch as controls. The
155 selected wild mustards were alpine rock cress (*Arabis alpine*, Aa), two accessions of shepherd's
156 purse (*Capsella bursa-pastoris*), Freiburg-1 (Cb-F) and Strasbourg-1 (Cb-S), pink shepherd's-purse
157 (*Capsella rubella*, Cr), watercress (*Nasturtium officinale*, No), and London rocket (*Sisymbrium irio*,
158 Si). Initially, we aimed to classify them as shade-avoider or shade-tolerant based on
159 photoacclimation responses. After germination and growth for 7 days under W, seedlings were
160 either kept under control W_{20} or transferred to lower light (W_4). Light curve analyses at day 1 after
161 the transfer already showed differential responses that served to classify the accessions in two
162 groups (Fig. 2). Similar to the shade-avoider At, seedlings of Cb-F, Cb-S and Cr showed a lowering
163 of the curve under W_4 conditions, whereas those of Aa, No and Si behaved as the shade-tolerant Ch

164 and showed virtually identical light curves under W_{20} and W_4 (Fig. 2A). ETR_m and alpha values
 165 also illustrated that the W_4 treatment led to decreased photosynthetic performance in At, Cb-F, Cb-S
 166 and Cr but not in Ch, Aa, No and Si (Fig. 2B, Supplemental Fig. S1). We next analyzed
 167 photoacclimation to increased irradiation quantifying Fv/Fm before or after transferring 7-day-old
 168 W_{20} -grown seedlings to W_{200} for 7 additional days. Again, At grouped together with the two
 169 accessions of Cb and with Cr as they acclimated much better to high PAR compared to the group
 170 formed by Ch, Aa, No and Si (Fig. 2C). Together, these photoacclimation results led to classify the
 171 former group as shade-avoiders, and the latter as shade-tolerant species.

172

173 **Photoacclimation responses can be uncoupled from shade-driven hypocotyl elongation**

174 Next, we investigated whether the classification of the selected mustard species as shade-
 175 avoider or shade-tolerant based on their photoacclimation features corresponded with their
 176 elongation response to low R:FR. After germination and growth for 3 days under W_{20} (R:FR=1.5-
 177 3.3), seedlings were either kept under W_{20} or transferred to FR-supplemented W_{20} (W_{20} +FR,
 178 R:FR=0.02) for 4 additional days, and then hypocotyl length was measured (Fig. 3). Similar to At,
 179 the Cb-F accession showed a strong hypocotyl elongation response, whereas Cb-S, Cr and No
 180 elongated moderately in response to low R:FR. By contrast, Ch, Aa and Si did not elongate in
 181 response to low R:FR (Fig. 3A). These results confirm that the elongation response to low R:FR
 182 cannot be fully predicted based on the photoacclimation phenotype of a particular accession.
 183 Nonetheless, accessions classified as shade-avoider based on their photoacclimation behavior (i.e.
 184 poor photoacclimation to decreased PAR but good photoacclimation to increased PAR) exhibit a
 185 range of elongation responses to low R:FR (i.e. from moderate to strong elongation), whereas plant
 186 species with a shade-tolerant photoacclimation responses display either no elongation or a mild
 187 shade-avoider phenotype in terms of hypocotyl elongation when exposed to low R:FR (e.g. No).

188 The shade-avoider or shade-tolerant elongation phenotype in response to low R:FR can be
 189 reversed by manipulating the levels of specific SAS regulators. Previous results have shown that At
 190 lines overexpressing *HY5* (*At-HY5ox*) display an attenuated hypocotyl response to low R:FR (Ortiz-
 191 Alcaide *et al*, 2019), whereas a similar but weaker response was observed in a quadruple mutant
 192 defective in all members of the photolabile PIF quartet (*At-pifq*) (Fig. 3B). Despite the different
 193 degrees of elongation response to low R:FR, these two lines showed photoacclimation responses to
 194 lower PAR very similar to those of wild-type (*At-WT*) controls (Fig. 4). Both light curves (Fig. 4A)
 195 and ETR_m values (Fig. 4B) were almost identical in *At-WT* plants and mutants hyposensitive to
 196 low R:FR. In the case of *C. hirsuta*, lines deficient in phyA (*Ch-sis1*) or HFR1 (*Ch-hfr1*) gain the
 197 ability to elongate when exposed to low R:FR (Molina-Contreras *et al*, 2019; Paulisic *et al*, 2021)

198 (Fig. 3B). In contrast to the shade-hyposensitive *At* mutants, the hypersensitive *Ch* mutant lines
 199 appeared to gain a partial shade-avoider phenotype in terms of photoacclimation to low PAR, as
 200 lower values of light curves (Fig. 4A) and ETRm (Fig. 4B) were observed under W_4 compared to
 201 W_{20} . However, photoacclimation to increased PAR (W_{200}) estimated from Fv/Fm values and also
 202 from chlorophyll levels (Molina-Contreras *et al*, 2019) was similar for *Ch*-WT, *Ch-sis1* and *Ch-hfr1*
 203 plants (Fig. 4C). We therefore concluded that manipulation of the plant ability to elongate in
 204 response to proximity shade hardly impacts their photoacclimation capacity, at least when plants are
 205 growing in the absence of the low R:FR signal.

206

207 **Activation of low R:FR signaling causes a decrease in pigment levels and photosynthetic** 208 **activity**

209 Low R:FR signals not only influence hypocotyl elongation but they are also known to reduce
 210 the contents of photosynthetic pigments (chlorophylls and carotenoids) in many plant species (Bou-
 211 Torrent *et al*, 2015; Cagnola *et al*, 2012; Molina-Contreras *et al*, 2019; Patel *et al*, 2013; Roig-
 212 Villanova *et al*, 2007). The reduction is observed in both elongating (*At*-WT) and non-elongating
 213 (*Ch*-WT) seedlings, but it is stronger in the former (Fig. 5). *C. hirsuta* mutants that gained the
 214 ability to elongate in response to shade, such as *Ch-sis1* and *Ch-hfr1*, also displayed stronger
 215 reductions in photosynthetic pigment contents relative to *Ch*-WT after low R:FR exposure (Fig. 5A)
 216 (Molina-Contreras *et al*, 2019). Conversely, *A. thaliana* mutants with a reduced ability to elongate
 217 in response to shade, such as *At-pifq* and *At-HY5ox* (Fig. 3B), showed attenuated reduction of
 218 pigment contents relative to *At*-WT when exposed to low R:FR (Fig. 5A).

219 To test whether decreases in photosynthetic pigment levels driven by simulated shade
 220 exposure might affect photosynthetic activity, we next measured Fv/Fm and ϕ PSII in seedlings
 221 grown either under W_{20} or under W_{20} +FR (Fig. 5B, Supplemental Fig. S2A). Indeed, low R:FR was
 222 found to result in decreased photosynthetic activity in the lines with strong pigment loss responses
 223 independently on the species (*At*-WT, *Ch-sis1* and *Ch-hfr1*). ETRm and alpha parameters also
 224 tended to be lower in W +FR-exposed *At*-WT, *Ch-sis1* and *Ch-hfr1* seedlings compared to W
 225 controls (Fig. 5C, Supplemental Fig. S2B). The effect of low R:FR on photosynthesis was much
 226 less dramatic in the rest of the lines (*At-pifq*, *At-HY5ox* and *Ch*-WT), which consistently displayed
 227 a reduced impact of W_{20} +FR exposure on their photosynthetic pigment levels (Fig. 5).

228 Proximity shade signals have also been found to impact photosynthesis at the level of gene
 229 expression. Analyses of low R:FR-triggered transcriptomic changes showed reduced levels of
 230 transcripts encoding photosynthesis-related proteins (e.g. enzymes involved in chlorophyll and
 231 carotenoid biosynthesis, components of the photosynthetic apparatus, and/or members of the carbon

232 fixation process) in several species, including alfalfa (Lorenzo *et al*, 2019), maize (Shi *et al*, 2019),
 233 tomato (Cagnola *et al*, 2012) and *A. thaliana* (Leivar *et al*, 2012). Interestingly, the changes in the
 234 expression of photosynthesis-related genes triggered by low R:FR are attenuated in the *At-pifq*
 235 mutant compared to *At-WT* seedlings (Fig. 6). This is particularly evident in the case of low R:FR-
 236 repressed photosynthetic genes (Fig. 6), suggesting that the PIF-mediated regulation of gene
 237 expression in response to low R:FR is instrumental for the observed changes in photosynthesis (Fig.
 238 5).

239

240 **Exposure of shade-avoider plants to low R:FR improves their photoacclimation to low PAR**

241 The observation that exposure of low R:FR caused a decreased in photosynthetic activity of
 242 *At-WT* seedlings and shade-hypersensitive *Ch* mutants prompted us to analyze whether this light
 243 signal may also cause changes in chloroplast ultrastructure. Cotyledons from *At-WT* seedlings
 244 germinated and grown for 2 days under W_{20} and then either kept in W_{20} or transferred to $W_{20}+FR$
 245 for 5 additional days were collected and used for transmission electron microscopy (TEM).
 246 Chloroplasts from low R:FR-exposed samples were found to exhibit larger grana stacks and contain
 247 less and smaller plastoglobules compared to W -grown controls (Fig. 7). Interestingly, similar
 248 changes are associated to low PAR photoacclimation (Lichtenthaler, 2007; Rozak *et al*, 2002;
 249 Wood *et al*, 2018). We therefore reasoned that exposure to low R:FR in the absence of any light
 250 intensity change might trigger responses to anticipate a foreseeable shading involving a decrease in
 251 PAR. To test this hypothesis, we analyzed light curves of *WT* and mutant seedlings grown in either
 252 W_{20} or $W_{20}+FR$ and then transferred to lower PAR (W_4) for 3 days (Fig. 8). Pre-exposure of *At-WT*
 253 seedlings to low R:FR ($W_{20}+FR$) resulted in a strongly attenuated reduction in ETR_m after their
 254 transfer to lower PAR (Fig. 8A). By contrast, *At* mutants with reduced SAS elongation responses
 255 also lost the response to low R:FR in terms of improved photoacclimation to lower PAR (W_4) (Fig.
 256 8A). Pre-treatment with $W_{20}+FR$ had virtually no effect on the photoacclimation of *Ch-WT*
 257 seedlings to lower PAR (W_4) but caused a slight but significant improvement of ETR_m in shade-
 258 hypersensitive *Ch* mutants at day 1 after transfer to W_4 (Fig. 8A). When analyzing photoacclimation
 259 to higher PAR, pre-exposure of *At-WT* or *Ch-WT* seedlings to $W_{20}+FR$ resulted in no improvement
 260 compared to W_{20} -grown controls (Fig. 8B). If anything, *Ch-WT* seedlings grown under $W_{20}+FR$
 261 photoacclimated worse than W_{20} -grown seedlings when exposed to higher light intensity (Fig. 8B).

262 The battery of mustards that grouped together with *At* in terms of photoacclimation responses
 263 (*Cb-F*, *Cb-S* and *Cr*) (Fig. 2, Supplemental Fig. S1) also showed improved photoacclimation to
 264 reduced PAR when pre-exposed to low R:FR, whereas the simulated shade signal did not have an
 265 effect on those clustered with *Ch* (*Aa*, *No* and *Si*) (Fig. 8A). This low R:FR-dependent phenotype

266 was independent of the growing light intensity and photoperiod, as it was also observed in At-WT
267 seedlings growing under W_{200} or $W_{200}+FR$ for 8 h or 16 h a day (i.e., under long day or short day
268 conditions, respectively) and then transferred to W_{15} (Supplemental Fig. S3). Because both the
269 response of shade-avoider plants to low R:FR and the acclimation to low light involve a reduced
270 respiration rate to cope with the limited generation of photoassimilates and hence contribute to
271 carbon balance (Cagnola *et al*, 2012)(Casal 2013), we next measured changes in respiration in
272 whole wild-type At and Ch seedlings exposed or not to low R:FR and then transferred to reduced
273 PAR (Supplemental Fig. S4). In W_{20} controls, respiration (estimated as total oxygen consumption in
274 darkness) was reduced in At seedlings when they were moved to W_4 . When exposed to $W_{20}+FR$,
275 however, respiration was already lower and did not significantly change after transferring to lower
276 PAR. By contrast, Ch seedlings showed similar respiration values in all conditions (Supplemental
277 Fig. S4). Based on these data we conclude that detection and transduction of low R:FR signals not
278 only allows shade-avoider plants to overgrow their neighbors but also to pre-adapt their
279 photosynthetic and respiratory machinery to foreseeable conditions of actual shading involving
280 reduced PAR. By contrast, shade-tolerant plants have a better adapted capacity to grow under
281 reduce PAR and do not seem to use the low R:FR signal.

282

283

284 **DISCUSSION**

285 Plants have been traditionally classified as shade avoider and tolerant based mostly on their
286 natural habitat, although virtually all plants are exposed to at least some degree of shade during
287 their lifetime. As an ecological concept, shade tolerance refers to the capacity of a given plant to
288 tolerate low light levels, but it is also associated with a wide range of traits, including phenotypic
289 plasticity to optimize light capture (Valladares & Niinemets, 2008). Analyzing a range of caulescent
290 herbs, it was suggested that the elongation response upon exposure to low R:FR was dependent on
291 the shade habit, the shade-avoiders elongating the most and the shade-tolerant showing a mild or no
292 elongation response (Smith, 1982). Indeed, elongation might not be the best solution for plants that
293 spend all their lives under a canopy or permanently shaded by other plants. Another important
294 parameter to ascertain the degree of shade tolerance of a plant is photoacclimation capacity, which
295 is essential for plant fitness in environments with changing light input conditions (e.g., those where
296 the growth of nearby plants may suddenly compromise access to light). By taking into account both
297 parameters (the hypocotyl elongation response and the capacity to acclimate to low or high PAR),
298 here we analyzed the shade tolerance of several Brassicaceae species, including the closely related
299 mustard model systems *A. thaliana* and *C. hirsuta*. As a rule of thumb, we observed that *C. hirsuta*

300 and other species showing a good photoacclimation response to lower PAR (and badly performing
301 after transfer to higher PAR) showed a poor or null elongation response to low R:FR (Fig. 2, 3).
302 Mustards such as *A. thaliana* that photoacclimated poorly to lower PAR but better to higher PAR
303 tended to more conspicuously elongate their hypocotyls in response to low R:FR, but there were
304 exceptions of poorly elongating species such as *Nasturtium officinale* (Fig. 2, 3). Furthermore,
305 mutation of genes encoding SAS regulators can dramatically change the elongation response to low
306 R:FR without improving the photoacclimation phenotype (Fig. 4). Together, these results confirm
307 that the capacity for photosynthetic acclimation to changing irradiance is a species-specific trend
308 (Bailey *et al.*, 2001) and a reliable indicator of shade tolerance. The shade-induced hypocotyl
309 elongation response should only be used as a complementary phenotype to classify a plant as shade-
310 tolerant (badly adapted to higher PAR exposure, well adapted to live under lower PAR and poorly
311 responsive to low R:FR) or shade-avoider (well adapted to higher PAR, poor performers under
312 lower PAR that elongate when exposed to low R:FR).

313 Our results also unveiled that an activation of low R:FR signaling in shade-avoider species
314 such as *A. thaliana* (At-WT) and shade-tolerant *C. hirsuta* plants with mutations causing low R:FR
315 hypersensitivity (Ch-*sis1* and Ch-*hfr1*) regulated photosynthesis at multiple levels. We confirmed
316 that exposure to W+FR caused a substantial decrease in the levels of photosynthetic pigments
317 (chlorophylls and carotenoids) in these lines (Bou-Torrent *et al.*, 2015; Molina-Contreras *et al.*,
318 2019; Paulisic *et al.*, 2021; Roig-Villanova *et al.*, 2007) and proved that the changes had a direct
319 impact on decreasing photosynthetic activity (Fig. 5). Low R:FR treatments are known to trigger
320 changes in gene expression within minutes (Kohnen *et al.*, 2016). These changes, which are often
321 instrumental for altering rapid growth responses, such as hypocotyl or petiole elongation, are
322 usually mediated by PIFs (Cifuentes-Esquivel *et al.*, 2013; de Wit *et al.*, 2015; Galstyan *et al.*, 2011;
323 Gallemi *et al.*, 2017; Hornitschek *et al.*, 2009). PIFs were also found to regulate longer-term changes
324 in gene expression such as those affecting photosynthetic genes (Fig. 6). Because loss of PIFQ
325 function in the *At-pifq* mutant resulted in a much attenuated response to W+FR compared to At-WT
326 in terms of photosynthetic gene expression (Fig. 6) but it also prevented photosynthetic pigment and
327 activity loss (Fig. 5), we propose that stabilization of PIFQ proteins following low R:FR exposure
328 triggers a reprogramming of photosynthesis-related gene expression that eventually results in lower
329 pigment levels and reduced photosynthetic activity. Based on the results obtained with other
330 mutants (Fig. 5), we speculate that this signaling network is further influenced by factors such as
331 HFR1 and HY5, which prevent PIF binding to target genes by heterodimerization (Hornitschek *et al.*
332 *et al.*, 2009) or competition for promoter binding sites (Toledo-Ortiz *et al.*, 2014), respectively.

333 Concomitant with the described molecular and physiological changes, we discovered that low
334 R:FR treatment of At-WT seedlings triggered ultrastructural changes in the chloroplast
335 endomembrane systems resembling those occurring after transfer to low PAR (Fig. 7). Grana with
336 more thylakoid layers and increased thickness were observed in the chloroplasts of At seedlings
337 exposed to simulated shade. By contrast, chloroplasts from tobacco (*Nicotiana tabacum*) leaves that
338 received end-of-day-FR treatments (considered to induce similar shade responses as low R:FR)
339 showed fewer thylakoid layers per granum but more small grana spread throughout the chloroplast
340 compared to end-of-day R controls (Kasperbauer & Hamilton, 1984). While these differences in
341 chloroplast ultrastructure might derive from distinct treatments being applied to diverse species,
342 both solutions likely contribute to optimize photosynthesis in the shade, when relatively less
343 photons would strike a leaf. Indeed, leaves that develop under low PAR have chloroplasts with less
344 plastoglobules (which are derived from thylakoid membranes) and more thylakoids per granum
345 (Rozak et al., 2002; Lichtenthaler, 2007; Wood et al., 2018). Based on these results, we suggest that
346 the chloroplast ultrastructural changes observed in At-WT plants grown under low R:FR are most
347 likely aimed to acclimate their photosynthetic machinery to perform better under low PAR by, for
348 instance, allowing a more efficient energy transfer. In agreement, pre-treatment with low R:FR
349 improved photoacclimation to low PAR of At-WT seedlings but had no effect in At mutants
350 defective in low R:FR signaling (Fig. 8). Further experiments showed that the observed positive
351 effect of low R:FR exposure for acclimation to low PAR can be observed in At-WT plants growing
352 under different light conditions (Supplemental Fig. S3) and in other shade-avoider Brassicaceae
353 (Cb-F, Cb-S and Cr), but not in shade-tolerant species such as Ch, Aa, No and Si (Fig. 8A).

354 At low irradiances, a proper balance between carbon allocation to growth and to respiration is
355 important to meet the challenges associated with a shade environment. Wild-type At (shade-
356 avoider) but not Ch (shade-tolerant) seedlings showed a drop in dark respiration when irradiation
357 was reduced (Supplemental Fig. S4), likely to reduce carbon loss for a better carbon balance. This
358 adaptive mechanism might contribute to explain why shade-avoider and shade-tolerant species
359 appear to show little or no differences in carbon balance under low light conditions (Pons &
360 Poorter, 2014; Sterck *et al*, 2013). Similar to that observed for photosynthetic activity (Fig. 8), the
361 respiration drop observed in At-WT seedlings was attenuated by pre-exposure to low R:FR
362 (Supplemental Fig. S4). Interestingly, there is evidence for the specific activation/deactivation of
363 respiratory pathways by the phytochrome system at different levels (Igamberdiev *et al*, 2014; Ribas-
364 Carbo *et al*, 2008). Regardless of the signaling pathway connecting low R:FR perception to reduced
365 photosynthesis and respiration, this is likely part of an anticipation mechanism for shade-avoider
366 plants to prepare for the foreseeable reduction in PAR associated with shading. Indeed, low R:FR

367 signals are perceived before actual shading takes place and light becomes limiting, and hence they
 368 are considered to act as a warning signal that shading might occur (Casal, 2013; Martinez-Garcia *et*
 369 *al.*, 2010). When shade-avoider plants such as *A. thaliana* and most crops (including tomato, cereals,
 370 or legumes) grow among taller plants or in a forest understory, they will use the low R:FR signals
 371 coming from a closing canopy to elongate (to overgrow its neighbors) but also to readapt its
 372 photosynthetic and respiratory machinery to low PAR before actual shading takes place. By
 373 contrast, shade-tolerant plants are adapted to grow under dim light and hence photoacclimation to
 374 low PAR is hardly improved even when hypersensitive mutants that show shade-avoider responses
 375 in terms of elongation (Fig. 3) and photosynthesis (Fig. 6) are pre-exposed to low R:FR (Fig. 8).

376 While the observed decrease in respiration and photosynthetic pigment and activity levels in
 377 shade-avoider plants appears to be part of the anticipation mechanism to an eventual reduction in
 378 PAR, a too committed response might be detrimental if light conditions change (e.g., if shading
 379 does not occur or shade plants become exposed again to direct sunlight). We have previously shown
 380 that a compensation mechanism exist that represses the response to low R:FR when the
 381 photosynthetic capacity of chloroplasts is compromised (Ortiz-Alcaide *et al.*, 2019). The retrograde
 382 (i.e. chloroplast-to-nucleus) pathway that adapts low R:FR perception and signaling to the
 383 photosynthetic status of the plant involves the antagonistic factors PIFs and HY5, which also
 384 participate in retrograde signaling when underground seedlings are illuminated and start their
 385 photomorphogenic (i.e. photosynthetic) development (Martin *et al.*, 2016; Ortiz-Alcaide *et al.*, 2019;
 386 Ruckle *et al.*, 2007; Xu *et al.*, 2016). The balance of positive and negative regulators together with
 387 the chloroplast-mediated control of SAS likely contribute to prevent an excessive response to shade,
 388 hence preventing photooxidative damage (resulting from light intensity exceeding the
 389 photosynthetic capacity of the plant) and facilitating the return to high R:FR conditions if the low
 390 R:FR signal disappears (e.g. if a commitment to the shade-avoidance lifestyle is unnecessary).
 391 Together, our work demonstrates that regulation of photosynthetic (chloroplast) performance is both
 392 an output and an input of the response of plants to shade. Our results therefore contribute to a better
 393 understanding of how plants respond to shade, a knowledge that will contribute to optimally grow
 394 crop plants closer together or/and under canopies (e.g., in intercropping settings).

395

396

397 **MATERIALS AND METHODS**

398 **Plant material and growth conditions**

399 Alpine rock cress (*Arabis alpina*, *pep1-1* mutant) (Wang *et al.*, 2009), *Arabidopsis*
 400 (*Arabidopsis thaliana*, Col-0 accession), hairy bittercress (*Cardamine hirsuta*, Oxford, Ox

401 accession) (Molina-Contreras *et al*, 2019), shepherd's purse (*Capsella bursa-pastoris*, accessions
402 Strasbourg-1, Str-1 and Freiburg-1, Fre-1), pink shepherd's-purse (*Capsella rubella*) and London
403 rocket (*Sisymbrium irio*) plants were grown in the greenhouse under long-day photoperiods (16 h
404 light and 8 h dark) to produce seeds, as described (Gallemi *et al*, 2017). Seeds of *C. bursa-pastoris*
405 were collected by Ruben Alcazar (University of Barcelona, Spain) from wild populations in
406 Strasbourg (France, coordinates: 48.612436, 7.767881; Str-1) and Freiburg (Germany, coordinates:
407 47.994945, 7.861979; Fre-1). Seeds of *Capsella rubella*, collected from wild populations in Crete
408 (Greece, coordinates 35.29, 24.42; accession 879) were previously described (Koenig *et al*, 2019).
409 Seeds of *Sisymbrium irio* were collected from wild populations in Bellaterra (Barcelona, Spain,
410 coordinates: 41.497731, 2.109558). Seeds of watercress (*Nasturtium officinale*) were provided by a
411 seed company (www.semillasfito.es). *A. thaliana* and *C. hirsuta* mutant and transgenic lines were
412 previously available in our laboratories (Molina-Contreras *et al*, 2019; Ortiz-Alcaide *et al*, 2019;
413 Paulisic *et al*, 2021).

414 For the light acclimation experiments seedlings were germinated and grown in Petri dishes
415 containing solid medium without sucrose (0.5x MS-): 2.2 g/L MS basal salt mixture (Duchefa), 1%
416 (w/v) agar, 0.25 g/L 2-(*N*-morpholino)ethanesulfonic acid -MES- (Sigma Aldrich), pH 5.7). Normal
417 light conditions refer to white light (W) produced by cool-white vertical fluorescent tubes of a
418 photosynthetic photon flux density in the PAR region (PPFD) of 20-24 $\mu\text{mol m}^{-2} \text{s}^{-1}$ (W_{20}) with a
419 R:FR of 1.5-3.3. Low light and high light conditions corresponded to W of PPFD of 4 (W_4) and 200
420 (W_{200}) $\mu\text{mol m}^{-2} \text{s}^{-1}$, respectively, produced by horizontal fluorescent tubes. Low R:FR treatment
421 was produced by supplementing W_{20} with FR ($W_{20}+\text{FR}$). FR was emitted from a GreenPower LED
422 module HF far-red (Philips), providing a R:FR of 0.02 (Martinez-Garcia *et al*, 2014). For the light
423 acclimation experiments shown in Supplemental Fig. S3, seedlings were germinated and grown in
424 Petri dishes, as previously described, but exposed to long-day (LD, 16 h light / 8 h darkness) or
425 short-day (SD, 8 h light / 16 h darkness) photoperiods. The light part of the photoperiod was
426 produced by cool-white horizontal fluorescent tubes of 200-210 $\mu\text{mol m}^{-2} \text{s}^{-1}$ of PPFD (W_{200}) with
427 R:FR of 2-3.5). In that case, low light conditions corresponded to values of 15 $\mu\text{mol m}^{-2} \text{s}^{-1}$ PPFD
428 (W_{15}). In this set-up, low R:FR treatment was produced by supplementing W_{200} with the same FR
429 lamps described above ($W_{200}+\text{FR}$), obtaining a R:FR of 0.2-0.25. Light fluence rates were measured
430 with a Spectrosense2 meter (Skye Instruments Ltd), which provides PPFD (400–700 nm), and
431 photon flux density in 10 nm windows of R (664–674 nm) and FR (725–735 nm) regions to
432 calculate the R:FR (Martinez-Garcia *et al*, 2014). Full spectra photon distribution of W and W+FR
433 treatments have been described elsewhere (Molina-Contreras *et al*, 2019).

434

435 **Measurement of hypocotyl length**

436 For hypocotyl measurement, about 30 seeds of each genotype were germinated and grown on
 437 plates containing 0.5x MS- solid media. For quantification of hypocotyl length, at least 20 seedlings
 438 were analyzed with the FIJI-ImageJ software (Schindelin *et al*, 2012), as described (Roig-Villanova
 439 *et al*, 2019). All experiments were repeated at least three times with consistent results. Hypocotyl
 440 measurements from all the different experiments were averaged.

441

442 **Photosynthetic measurements and pigment quantification**

443 Whole seedlings were harvested, ground in liquid nitrogen, and the resulting powder was used
 444 for quantification of chlorophylls and carotenoids either spectrophotometrically or by HPLC as
 445 described (Bou-Torrent *et al*, 2015). Chlorophyll fluorescence measurements were carried out on
 446 seedlings using a MAXI-PAM fluorometer (Heinz Walz GmbH) as described (Molina-Contreras *et*
 447 *al*, 2019). Briefly, for every measurement the whole cotyledons of 7 seedlings were considered.
 448 Effective quantum yield of photosystem II (PSII) under growth light, ϕPSII , was measured as
 449 $\Delta F/F_m'$, where ΔF corresponds to $F_m' - F$ (the maximum minus the minimum fluorescence of light-
 450 exposed plants). Maximum quantum yield of PSII, F_v/F_m , was calculated as $(F_m - F_o)/F_m$, where
 451 F_m and F_o are respectively the maximum and the minimum fluorescence of dark-adapted samples.
 452 For dark acclimation, plates were incubated for at least 30 minutes in darkness to allow the full
 453 relaxation of photosystems. Light curves were constructed with 10 incremental steps of actinic
 454 irradiance (E ; 0, 20, 55, 110, 185, 280, 395, 530, 610, 700 $\mu\text{mol photons}\cdot\text{m}^{-2}\cdot\text{s}^{-1}$ of PPFD). For each
 455 step, ϕPSII was monitored every minute and electron transport rate (ETR) was calculated as
 456 $E \times \phi\text{PSII} \times 0.84 \times 0.5$ (where 0.84 is light absorptance by an average green leaf and 0.5 is the fraction
 457 of absorbed quanta available for PSII). The light response and associated parameters ETR_m
 458 (maximum electron transport rate) and α (photosynthetic rate in light-limited region of the light
 459 curve) were characterized by fitting iteratively the model of the rETR versus E curves using MS
 460 Excel Solver (Platt *et al*, 1980). The fit was very good in all the cases ($r > 0.98$).

461

462 **Respiration measurements**

463 Seedlings were germinated and grown on 0.5x MS- plates, as described (Supplemental Fig.
 464 S4). Before the measurements, seedlings were placed in the dark for about 30 minutes to avoid
 465 light-enhanced dark respiration. Five to ten seedlings were then collected, immediately weighed,
 466 and placed into the respiration cuvette containing the respiration buffer (30 mM MES pH 6.2, 0.2
 467 mM CaCl_2). Oxygen uptake rates were measured in darkness using a liquid-phase Clark-type

468 oxygen electrode (Rank Brothers Ltd) as previously described (Flores-Sarasa *et al*, 2009) at a
469 constant temperature of 23°C.

470

471 **Microarray data analyses**

472 Microarray data corresponding to *A. thaliana* Col-0 (At-WT) and *At-pifq* seedlings exposed
473 to low-R:FR for 0, 1, 3 and 24 h (Leivar *et al*, 2012) were analyzed to select for differentially-
474 expressed genes (DEGs) specifically related to photosynthesis. The reported list of DEGs was
475 further filtered using cut-offs of FDR <0.05 and log₂-transformed fold change (log₂FC) higher than
476 0.585 for upregulated genes and lower than -0.599 for downregulated genes. Then, photosynthesis-
477 related genes were identified by using the KEGG (Kyoto Encyclopedia of Genes and Genomes)
478 Mapper tool (Kanehisa & Sato, 2020).

479

480 **Transmission electron microscopy**

481 Transmission electron microscopy (TEM) was carried out as described (Flores-Perez *et al*,
482 2008). Chloroplast features in the pictures were quantified by using the FIJI-ImageJ software
483 (Schindelin *et al*, 2012).

484

485

486 **ACCESSION NUMBERS**

487 Sequence data from this article can be found in the EMBL/Genbank and *Cardamine hirsuta*
488 genetic and genomic resource (<http://chi.mpipz.mpg.de>) data libraries under the following accession
489 numbers: *AT1G02340* (*AtHFR1*), *AT5G11260* (*AtHY5*), *AT2G20180* (*AtPIF1*), *AT1G09530*
490 (*AtPIF3*), *AT2G43010* (*AtPIF4*), *AT3G59060* (*AtPIF5*), *CARHR001660* (*ChHFR1*) and
491 *CARHR009540* (*SIS1/ChPHYA*).

492

493 **SUPPLEMENTAL DATA**

494 **Supplemental Figure S1.** Alpha values calculated from the light curves shown in Fig 2A.

495 **Supplemental FigureS2.** Activation of low R:FR signaling reduces photosynthetic activity.

496 **Supplemental Figure S3.** Pre-exposure to low R:FR improves photoacclimation to lower PAR in
497 *Arabidopsis thaliana* plants grown under photoperiods.

498 **Supplemental Figure S4.** Exposure to low R:FR differentially impacts respiration rate of shade-
499 avoider and shade-tolerant plants.

500

501 **ACKNOWLEDGEMENTS**

502 We thank M^a Rosa Rodríguez (CRAG) for technical support, and George Coupland (MPI for
503 Plant Breeding Research, Cologne, Germany), Rubén Alcazar (Universitat de Barcelona, Spain) and
504 Ignacio Rubio (CRAG) for providing mustard seeds.

505

506

507 **COMPETING INTERESTS**

508 The authors declare no competing interests.

509 **FIGURE LEGENDS**

510

511 **Figure 1. *Arabidopsis thaliana* and *Cardamine hirsuta* show antagonistic photoacclimation**
512 **responses to higher and lower PAR. (A)** Light curves of *A. thaliana* (At) and *C. hirsuta* (Ch)
513 seedlings germinated and grown under white light of $20 \mu\text{mol}\cdot\text{m}^{-2}\cdot\text{s}^{-1}$ PPFD (W_{20}) for 7 days and
514 then either kept under W_{20} or transferred to either 200 (W_{200}) or 4 (W_4) $\mu\text{mol}\cdot\text{m}^{-2}\cdot\text{s}^{-1}$ PPFD for 3
515 more days. Values represent the mean and standard error of $n=3$ plants for treatment. **(B)** Maximum
516 relative electron transport rate (ETR_m) and photosynthetic rate in the light-limited region of the
517 light curve (alpha) calculated from the curves shown in **A**. Asterisks mark statistically significant
518 changes (t test * $P<0.05$, ** $P<0.01$) in W_4 or W_{200} relative to W_{20} . **(C)** Maximum photochemical
519 efficiency of PSII in the dark-adapted state (F_v/F_m) and effective quantum yield calculated at
520 growth light (Φ PSII) of seedlings germinated and grown for 7 days under W_{20} and then transferred
521 to either W_{200} or W_4 for 7 more days. Data were taken at 0, 3 and 7 days after the transfer. Values
522 are mean and standard error of $n=7$ seedlings per treatment. Black asterisks mark statistically
523 significant differences between At and Ch at each time point (t test * $P < 0.05$ and ** $P < 0.01$). Red
524 asterisks indicate statistically significant differences between genotypes over time (two-way
525 ANOVA, **, $P<0.01$).

526

527 **Figure 2. Brassicaceae plants can be grouped with either *Arabidopsis thaliana* or *Cardamine***
528 ***hirsuta* based on their photoacclimation responses. (A)** Light curves of *Arabidopsis thaliana*
529 (At), *Capsella bursa-pastoris* (Cb-F and Cb-S), *Capsella rubella* (Cr), *Cardamine hirsuta* (Ch),
530 *Arabis alpina* (Aa), *Nasturtium officinale* (No), and *Sisymbrium irio* (Si) seedlings germinated and
531 grown under white light (W_{20}) for 7 days and then either kept under W_{20} or transferred to lower
532 PAR (W_4) for 1 more day. Values represent the mean and standard error of $n=3$ plants for treatment.
533 **(B)** ETR_m values calculated from the curves shown in **A**. **(C)** F_v/F_m values of seedlings grown for
534 7 days under W_{20} and then transferred to higher PAR (W_{200}) for 7 more days. Mean and standard
535 error of $n=9$ seedlings per treatment are represented. Asterisks in **B** and **C** mark statistically
536 significant changes (t test, ** $P<0.01$) relative to W_{20} .

537

538 **Figure 3. The hypocotyl elongation response to low R:FR is plastic in Brassicaceae plants. (A)**
539 The indicated genotypes were germinated and grown under W_{20} for 3 days and then either kept
540 under W_{20} or transferred to low R:FR ($W_{20}+\text{FR}$) for 4 more days. Then, pictures were taken and
541 hypocotyl length was measured. **(B)** Hypocotyl length of the indicated mutants grown as indicated
542 in **A**. In both **A** and **B**, mean and standard error of measurements from at least 20 seedlings in $n=3$

543 independent experiments per treatment are represented. Asterisks mark statistically significant
544 changes in W_{20+FR} relative to W_{20} (t test, * $P<0.05$ and ** $P<0.01$).

545

546 **Figure 4. Mutations that alter sensitivity to low R:FR do not impact photoacclimation**

547 **responses. (A)** Light curves of *A. thaliana* and *C. hirsuta* wild-type and mutant seedlings
548 germinated and grown under W_{20} for 7 days and then either kept under W_{20} or transferred to lower
549 PAR (W_4) for 1 more day. Values represent the mean and standard error of $n=3$ plants for treatment.

550 **(B)** ETR_m values calculated from the curves shown in **A**. **(C)** Fv/Fm values and HPLC-determined
551 relative chlorophyll levels of seedlings grown for 7 days under W_{20} and then transferred to higher
552 PAR (W_{200}) for 7 more days. Mean and standard error of $n=9$ seedlings (Fv/Fm) or $n=3$ independent
553 pools (HPLC) per treatment are represented. Asterisks in **B** and **C** mark statistically significant
554 changes (t test, * $P<0.05$, ** $P<0.01$) relative to W_{20} .

555

556 **Figure 5. Activation of low R:FR signaling reduces photosynthetic pigment levels and activity.**

557 **(A)** The indicated genotypes were germinated and grown under W_{20} for 3 days and then either kept
558 under W_{20} or transferred to low R:FR (W_{20+FR}) for 4 more days. Then, the levels of photosynthetic
559 pigments (carotenoids and chlorophylls) were quantified spectrophotometrically. **(B)** Fv/Fm values
560 of seedlings germinated and grown as indicated in **A**. Lower pictures show false-color images in
561 wild-type seedlings. **(C)** ETR_m values of seedlings germinated and grown as indicated in **A**. Mean
562 and standard error of $n=3$ independent pools of seedlings (**A**) or $n=9$ seedlings (**B**, **C**) per treatment
563 are represented. Asterisks mark statistically significant changes in W_{20+FR} relative to W_{20} (t test, *
564 $P<0.05$).

565

566 **Figure 6. Exposure to low R/FR triggers changes in photosynthetic gene expression that are**

567 **attenuated in the hyposensitive *At-pifq* mutant.** Data were extracted from a publicly available
568 experiment (Leivar *et al*, 2012). *At*-WT and *At-pifq* lines were germinated and grown under 19
569 $\mu\text{mol}\cdot\text{m}^{-2}\cdot\text{s}^{-1}$ PAR white light (W_{20} , R:FR of 6.48) for 2 days and exposed to low R:FR (W_{20+FR} ,
570 R:FR of 0.006) for 0, 1, 3 or 24 h. Plots represent the number of differentially expressed genes
571 (DEGs) either up- or down-regulated in W_{20+FR} vs. W_{20} that are involved in photosynthetic
572 pigment biosynthesis (KEGG pathways ath00906 and ath00860), photosynthesis (ath00195 and
573 ath00196), and carbon fixation (ath00710).

574

575 **Figure 7. Low R:FR triggers ultrastructural changes in *A. thaliana* chloroplasts.** *At*-WT seeds

576 were germinated and grown under W_{20} for 2 days and then either kept under W_{20} or transferred to

577 low R:FR (W_{20+FR}) for 5 more days. Cotyledons were then used for TEM analysis of chloroplast
578 ultrastructure. Representative pictures at different scales (numbers indicate μm) are shown.
579 Boxplots show quantification of the indicated parameters from the images. Boxes show the values
580 between the upper and the lower quartile, the cross represents the mean and the horizontal line the
581 median. Whiskers (the upper and lower extremes) and circles represent single data and the ones
582 located outside of the whiskers limit are the outliers (data with the same numerical value are
583 visualized as a single point). For quantifying grana thickness, all the distinguishable structures were
584 used (W_{20} $n=30$, W_{20+FR} $n=20$). For quantifying grana layers, 4 major grana complexes from
585 higher magnifications were measured. For quantifying the number of plastoglobules, at least 6
586 individual chloroplasts for each treatment were used. Plastoglobule area was measured for all the
587 plastoglobules (W_{20} $n=87$, W_{20+FR} $n=22$). PG, plastoglobules. G, grana.

588

589 **Figure 8. Pre-exposure to low R:FR improves the photoacclimation to low PAR in shade-**
590 **avoider plants. (A)** The indicated genotypes were germinated and grown under W_{20} for 3 days,
591 transferred to either W_{20} or W_{20+FR} for 4 days, and then exposed to W_4 . Mean and standard error of
592 ETR_m values at 0, 1, 2 and 3 days after transfer to W_4 are shown ($n=3$ seedlings per treatment).
593 Asterisks indicate statistically significant differences between treatments (W_{20} or W_{20+FR}) over
594 time (two-way ANOVA, * $P<0.05$, **, $P<0.01$). **(B)** Wild-type *A. thaliana* and *C. hirsuta* lines
595 were germinated and grown under W_{20} for 2 days, transferred to either W_{20} or W_{20+FR} for 5 days,
596 and then exposed to W_{200} for 7 more days. Fv/Fm values and HPLC-quantified chlorophyll levels
597 were determined. Mean and standard error of $n=7$ seedlings (Fv/Fm) or $n=3$ independent pools
598 (HPLC) per treatment are represented. Asterisks mark statistically significant differences between
599 values before and after exposure to W_{200} (t test, * $P<0.05$; ** $P<0.01$).

600

601

REFERENCES

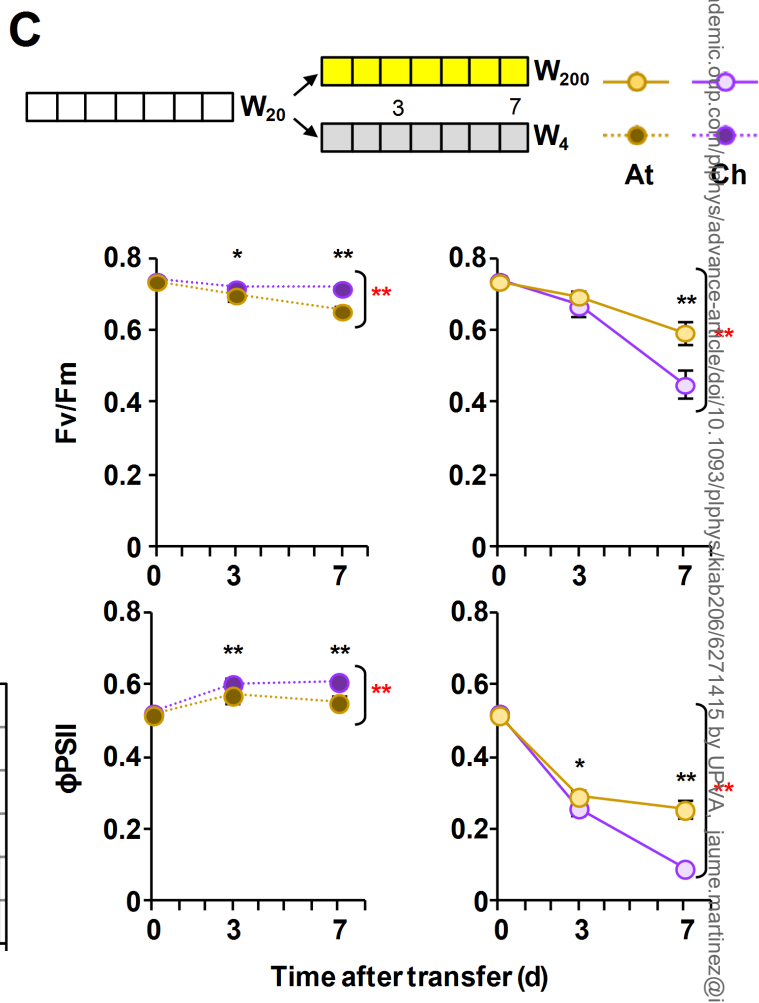
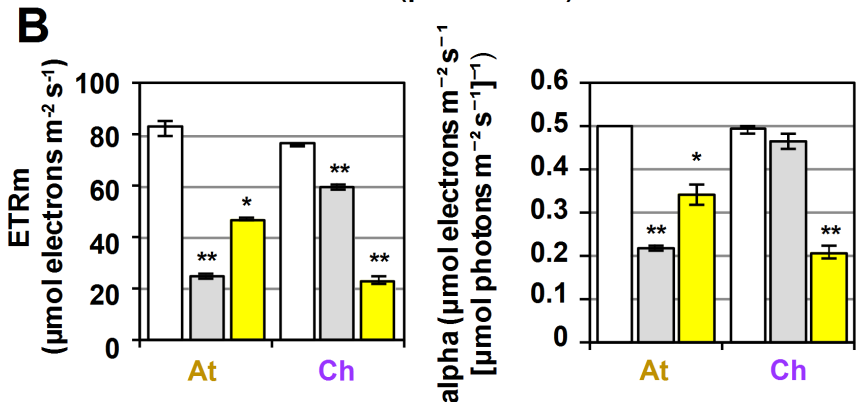
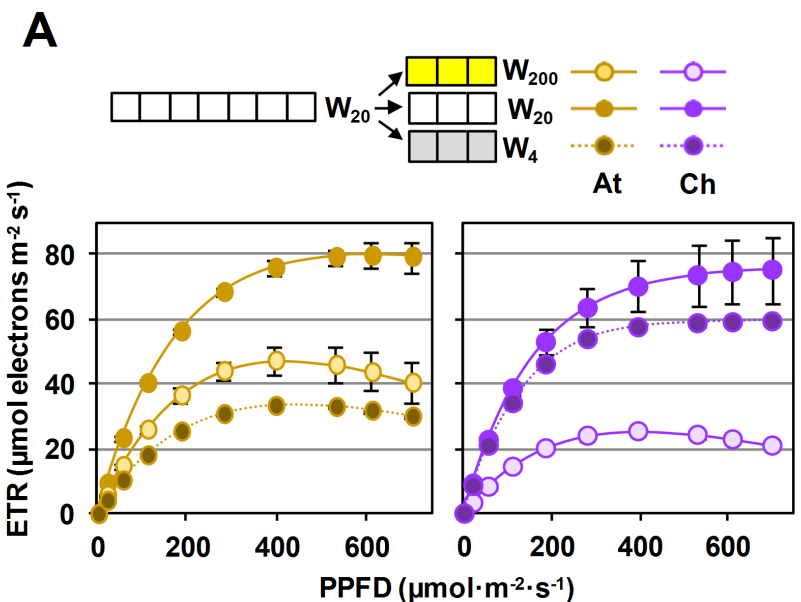
- 602
603 Bailey S, Walters RG, Jansson S, Horton P (2001) Acclimation of *Arabidopsis thaliana* to the light
604 environment: the existence of separate low light and high light responses. *Planta* **213**: 794-
605 801
- 606 Benkov MA, Yatsenko AM, Tikhonov AN (2019) Light acclimation of shade-tolerant and sun-
607 resistant *Tradescantia* species: photochemical activity of PSII and its sensitivity to heat
608 treatment. *Photosynth Res* **139**: 203-214
- 609 Bou-Torrent J, Toledo-Ortiz G, Ortiz-Alcaide M, Cifuentes-Esquivel N, Halliday KJ, Martinez-
610 Garcia JF, Rodriguez-Concepcion M (2015) Regulation of Carotenoid Biosynthesis by
611 Shade Relies on Specific Subsets of Antagonistic Transcription Factors and Cofactors. *Plant*
612 *Physiol* **169**: 1584-1594
- 613 Cagnola JJ, Ploschuk E, Benech-Arnold T, Finlayson SA, Casal JJ (2012) Stem transcriptome
614 reveals mechanisms to reduce the energetic cost of shade-avoidance responses in tomato.
615 *Plant Physiol* **160**: 1110-1119
- 616 Casal JJ (2013) Photoreceptor signaling networks in plant responses to shade. *Annu Rev Plant Biol*
617 **64**: 403-427
- 618 Cifuentes-Esquivel N, Bou-Torrent J, Galstyan A, Gallemi M, Sessa G, Salla Martret M, Roig-
619 Villanova I, Ruberti I, Martinez-Garcia JF (2013) The bHLH proteins BEE and BIM
620 positively modulate the shade avoidance syndrome in *Arabidopsis* seedlings. *The Plant*
621 *Journal* **75**: 989-1002
- 622 Ciolfi A, Sessa G, Sassi M, Possenti M, Salvucci S, Carabelli M, Morelli G, Ruberti I (2013)
623 Dynamics of the shade-avoidance response in *Arabidopsis*. *Plant Physiol* **163**: 331-353
- 624 de Wit M, Ljung K, Fankhauser C (2015) Contrasting growth responses in lamina and petiole
625 during neighbor detection depend on differential auxin responsiveness rather than different
626 auxin levels. *New Phytol* **208**: 198-209
- 627 Flores-Perez U, Sauret-Gueto S, Gas E, Jarvis P, Rodriguez-Concepcion M (2008) A mutant
628 impaired in the production of plastome-encoded proteins uncovers a mechanism for the
629 homeostasis of isoprenoid biosynthetic enzymes in *Arabidopsis* plastids. *Plant Cell* **20**:
630 1303-1315
- 631 Florez-Sarasa I, Ostaszewska M, Galle A, Flexas J, Rychter AM, Ribas-Carbo M (2009) Changes
632 of alternative oxidase activity, capacity and protein content in leaves of *Cucumis sativus*
633 wild-type and MSC16 mutant grown under different light intensities. *Physiol Plant* **137**:
634 419-426
- 635 Galstyan A, Cifuentes-Esquivel N, Bou-Torrent J, Martinez-Garcia JF (2011) The shade avoidance
636 syndrome in *Arabidopsis*: a fundamental role for atypical basic helix-loop-helix proteins as
637 transcriptional cofactors. *Plant J* **66**: 258-267
- 638 Gallemi M, Molina-Contreras MJ, Paulisic S, Salla-Martret M, Sorin C, Godoy M, Franco-Zorrilla
639 JM, Solano R, Martinez-Garcia JF (2017) A non-DNA-binding activity for the ATHB4
640 transcription factor in the control of vegetation proximity. *New Phytol* **216**: 798-813
- 641 Hay AS, Pieper B, Cooke E, Mandakova T, Cartolano M, Tattersall AD, Ioio RD, McGowan SJ,
642 Barkoulas M, Galinha C *et al* (2014) *Cardamine hirsuta*: a versatile genetic system for
643 comparative studies. *Plant J* **78**: 1-15
- 644 Hornitschek P, Lorrain S, Zoete V, Michielin O, Fankhauser C (2009) Inhibition of the shade
645 avoidance response by formation of non-DNA binding bHLH heterodimers. *EMBO J* **28**:
646 3893-3902
- 647 Igamberdiev AU, Eprintsev AT, Fedorin DN, Popov VN (2014) Phytochrome-mediated regulation
648 of plant respiration and photorespiration. *Plant Cell Environ* **37**: 290-299
- 649 Kanehisa M, Sato Y (2020) KEGG Mapper for inferring cellular functions from protein sequences.
650 *Protein Sci* **29**: 28-35

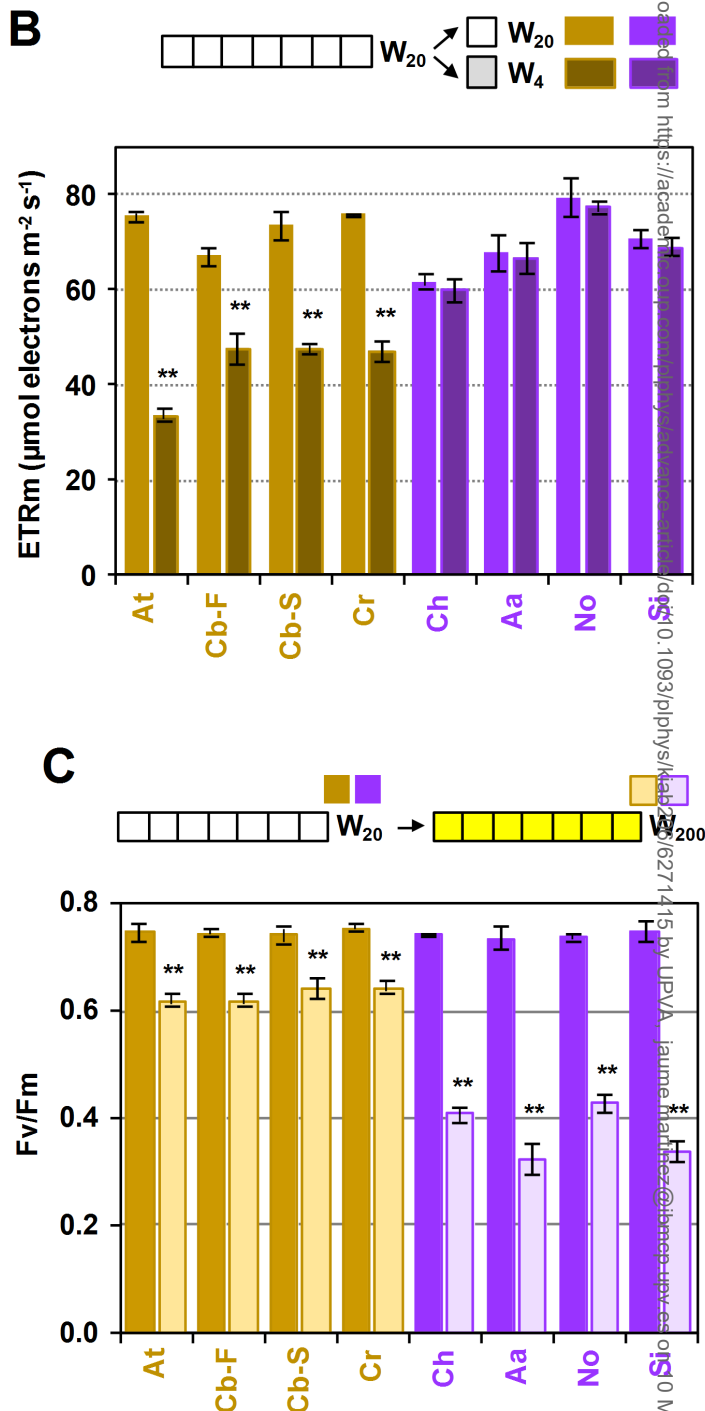
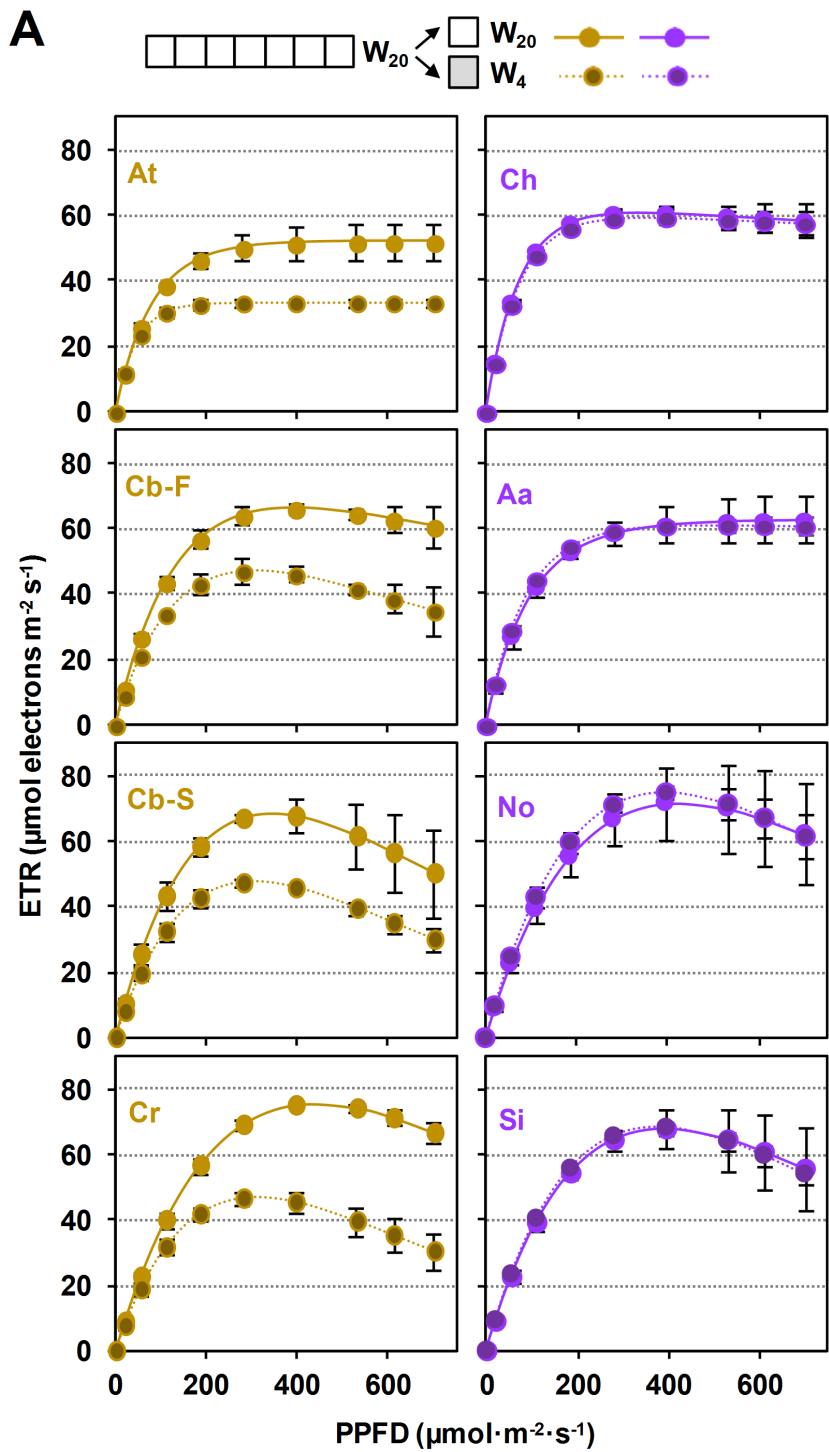
- 651 Koenig D, Hagmann J, Li R, Bemm F, Slotte T, Neuffer B, Wright SI, Weigel D (2019) Long-term
652 balancing selection drives evolution of immunity genes in *Capsella*. *Elife* **8**
- 653 Kohnen MV, Schmid-Siegert E, Trevisan M, Petrolati LA, Senechal F, Muller-Moule P, Maloof J,
654 Xenarios I, Fankhauser C (2016) Neighbor Detection Induces Organ-Specific
655 Transcriptomes, Revealing Patterns Underlying Hypocotyl-Specific Growth. *Plant Cell* **28**:
656 2889-2904
- 657 Leivar P, Tepperman JM, Cohn MM, Monte E, Al-Sady B, Erickson E, Quail PH (2012) Dynamic
658 antagonism between phytochromes and PIF family basic helix-loop-helix factors induces
659 selective reciprocal responses to light and shade in a rapidly responsive transcriptional
660 network in *Arabidopsis*. *Plant Cell* **24**: 1398-1419
- 661 Lichtenthaler HK (2007) Biosynthesis, accumulation and emission of carotenoids, alpha-tocopherol,
662 plastoquinone, and isoprene in leaves under high photosynthetic irradiance. *Photosynth Res*
663 **92**: 163-179
- 664 Lorenzo CD, Alonso Iserte J, Sanchez Lamas M, Antonietti MS, Garcia Gagliardi P, Hernando CE,
665 Dezar CAA, Vazquez M, Casal JJ, Yanovsky MJ *et al* (2019) Shade delays flowering in
666 *Medicago sativa*. *Plant J* **99**: 7-22
- 667 Martin G, Leivar P, Ludevid D, Tepperman JM, Quail PH, Monte E (2016) Phytochrome and
668 retrograde signalling pathways converge to antagonistically regulate a light-induced
669 transcriptional network. *Nat Commun* **7**: 11431
- 670 Martinez-Garcia JF, Galstyan A, Salla-Martret M, Cifuentes-Esquivel N, Gallemí M, Bou-Torrent J
671 (2010) Regulatory components of shade avoidance syndrome. *Advances in Botanical*
672 *Research* **53**: 65-116
- 673 Martinez-Garcia JF, Gallemi M, Molina-Contreras MJ, Llorente B, Bevilaqua MR, Quail PH (2014)
674 The shade avoidance syndrome in *Arabidopsis*: the antagonistic role of phytochrome a and
675 B differentiates vegetation proximity and canopy shade. *PLoS One* **9**: e109275
- 676 Molina-Contreras MJ, Paulisic S, Then C, Moreno-Romero J, Pastor-Andreu P, Morelli L, Roig-
677 Villanova I, Jenkins H, Hallab A, Gan X *et al* (2019) Photoreceptor Activity Contributes to
678 Contrasting Responses to Shade in *Cardamine* and *Arabidopsis* Seedlings. *Plant Cell* **31**:
679 2649-2663
- 680 Murchie EH, Horton P (1997) Acclimation of photosynthesis to irradiance and spectral quality in
681 British plant species: chlorophyll content, photosynthetic capacity and habitat preference
682 *Plant Cell Environ* **20**: 438-448
- 683 Ortiz-Alcaide M, Llamas E, Gomez-Cadenas A, Nagatani A, Martinez-Garcia JF, Rodriguez-
684 Concepcion M (2019) Chloroplasts modulate elongation responses to canopy shade by
685 retrograde pathways involving HY5 and ABA. *Plant Cell*
- 686 Patel D, Basu M, Hayes S, Majlath I, Hetherington FM, Tschaplinski TJ, Franklin KA (2013)
687 Temperature-dependent shade avoidance involves the receptor-like kinase ERECTA. *Plant J*
688 **73**: 980-992
- 689 Paulisic S, Qin W, Arora Veraszto H, Then C, Alary B, Nogue F, Tsiantis M, Hothorn M, Martinez-
690 Garcia JF (2021) Adjustment of the PIF7-HFR1 transcriptional module activity controls
691 plant shade adaptation. *EMBO J* **40**: e104273
- 692 Platt T, Gallegos CL, Harrison WG (1980) Photoinhibition of photosynthesis in natural
693 assemblages of marine phytoplankton. *Journal of Marine Research* **38**: 687-701
- 694 Pons TL, Poorter H (2014) The effect of irradiance on the carbon balance and tissue characteristics
695 of five herbaceous species differing in shade-tolerance. *Front Plant Sci* **5**: 12
- 696 Ptushenko OS, Ptushenko VV (2019) *Tradescantia*-based models: a powerful looking glass for
697 investigation of photoacclimation and photoadaptation in plants. *Physiol Plant* **166**: 120-133
- 698 Ribas-Carbo M, Giles L, Flexas J, Briggs W, Berry JA (2008) Phytochrome-driven changes in
699 respiratory electron transport partitioning in soybean (*Glycine max. L.*) cotyledons. *Plant*
700 *Biol (Stuttg)* **10**: 281-287

- 701 Roig-Villanova I, Bou-Torrent J, Galstyan A, Carretero-Paulet L, Portoles S, Rodriguez-
702 Concepcion M, Martinez-Garcia JF (2007) Interaction of shade avoidance and auxin
703 responses: a role for two novel atypical bHLH proteins. *The EMBO Journal* **26**: 4756-4767
704 Roig-Villanova I, Martinez-Garcia JF (2016) Plant Responses to Vegetation Proximity: A Whole
705 Life Avoiding Shade. *Front Plant Sci* **7**: 236
706 Roig-Villanova I, Paulisic S, Martinez-Garcia JF (2019) Shade Avoidance and Neighbor Detection.
707 *Methods Mol Biol* **2026**: 157-168
708 Rozak PR, Seiser RM, Wacholtz WF, Wise RR (2002) Rapid, reversible alterations in spinach
709 thylakoid appression upon changes in light intensity. *Plant Cell Environ* **25**: 421-429
710 Ruckle ME, DeMarco SM, Larkin RM (2007) Plastid signals remodel light signaling networks and
711 are essential for efficient chloroplast biogenesis in Arabidopsis. *Plant Cell* **19**: 3944-3960
712 Schindelin J, Arganda-Carreras I, Frise E, Kaynig V, Longair M, Pietzsch T, Preibisch S, Rueden
713 C, Saalfeld S, Schmid B *et al* (2012) Fiji: an open-source platform for biological-image
714 analysis. *Nat Methods* **9**: 676-682
715 Shi Q, Kong F, Zhang H, Jiang Y, Heng S, Liang R, Ma L, Liu J, Lu X, Li P *et al* (2019) Molecular
716 mechanisms governing shade responses in maize. *Biochem Biophys Res Commun* **516**: 112-
717 119
718 Smith H (1982) Light quality, photoperception, and plant strategy. *Annual Review of Plant*
719 *Physiology* **33**: 481-518
720 Sterck FJ, Duursma RA, Pearcy RW, Valladares F, Cieslak M, Weemstra M (2013) Plasticity
721 influencing the light compensation point offsets the specialization for light niches across
722 shrub species in a tropical forest understorey. *Journal of Ecology* **101**: 971-980
723 Toledo-Ortiz G, Johansson H, Lee KP, Bou-Torrent J, Stewart K, Steel G, Rodriguez-Concepcion
724 M, Halliday KJ (2014) The HY5-PIF regulatory module coordinates light and temperature
725 control of photosynthetic gene transcription. *PLoS Genet* **10**: e1004416
726 Valladares F, Niinemets U (2008) Shade Tolerance, a Key Plant Feature of Complex Nature and
727 Consequences. *Annual Review of Ecology, Evolution, and Systematics* **39**: 237-257
728 Wang R, Farrona S, Vincent C, Joecker A, Schoof H, Turck F, Alonso-Blanco C, Coupland G,
729 Albani MC (2009) PEP1 regulates perennial flowering in *Arabidopsis thaliana*. *Nature* **459**: 423-
730 427
731 Wood WHJ, MacGregor-Chatwin C, Barnett SFH, Mayneord GE, Huang X, Hobbs JK, Hunter CN,
732 Johnson MP (2018) Dynamic thylakoid stacking regulates the balance between linear and
733 cyclic photosynthetic electron transfer. *Nat Plants* **4**: 116-127
734 Xu X, Chi W, Sun X, Feng P, Guo H, Li J, Lin R, Lu C, Wang H, Leister D *et al* (2016)
735 Convergence of light and chloroplast signals for de-etiolation through ABI4-HY5 and
736 COP1. *Nat Plants* **2**: 16066
737 Yang C, Xie F, Jiang Y, Li Z, Huang X, Li L (2018) Phytochrome A Negatively Regulates the
738 Shade Avoidance Response by Increasing Auxin/Indole Acidic Acid Protein Stability. *Dev*
739 *Cell* **44**: 29-41 e24

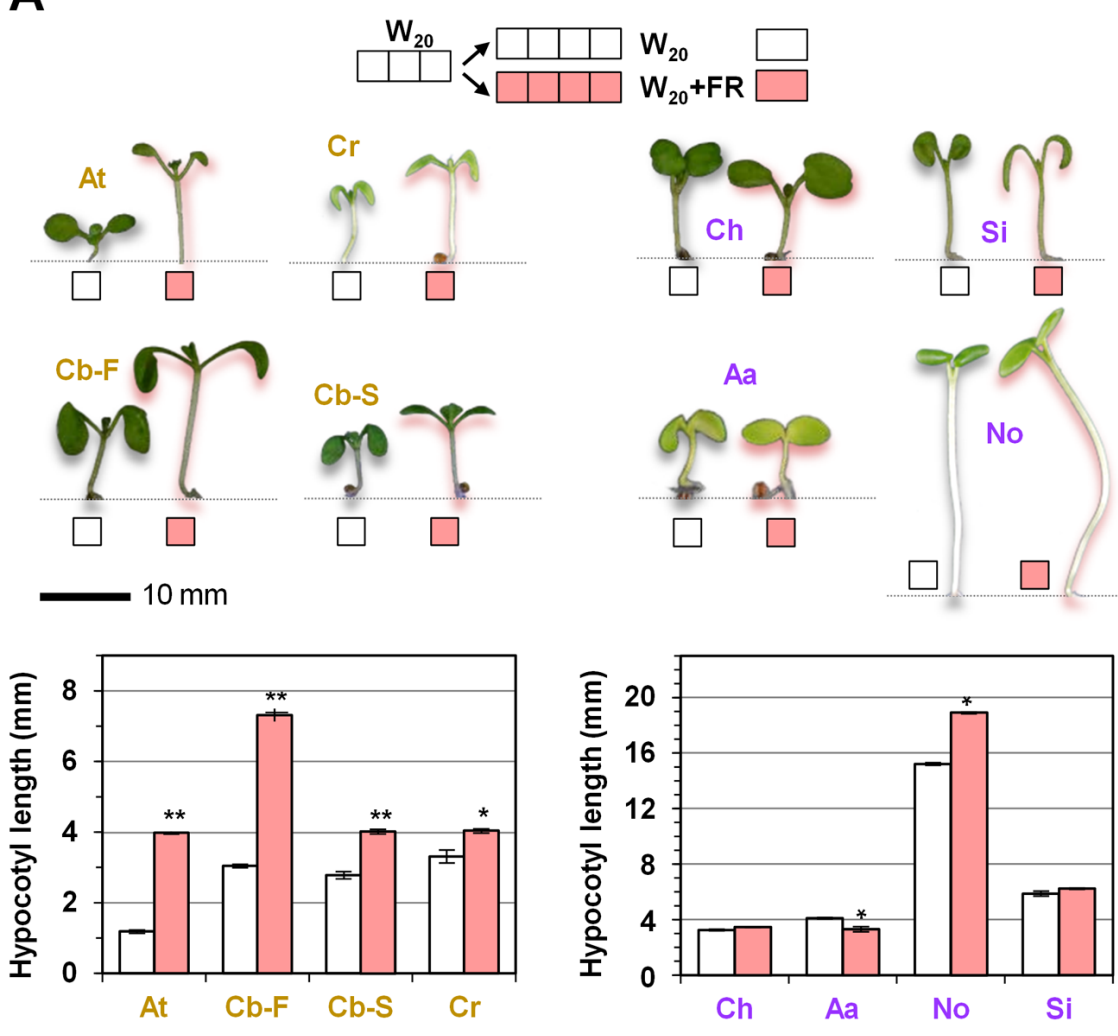
740

741

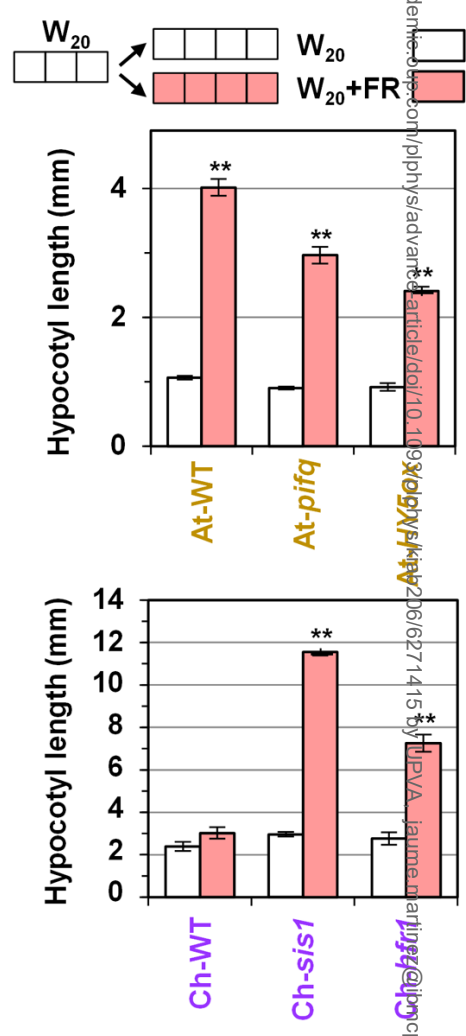


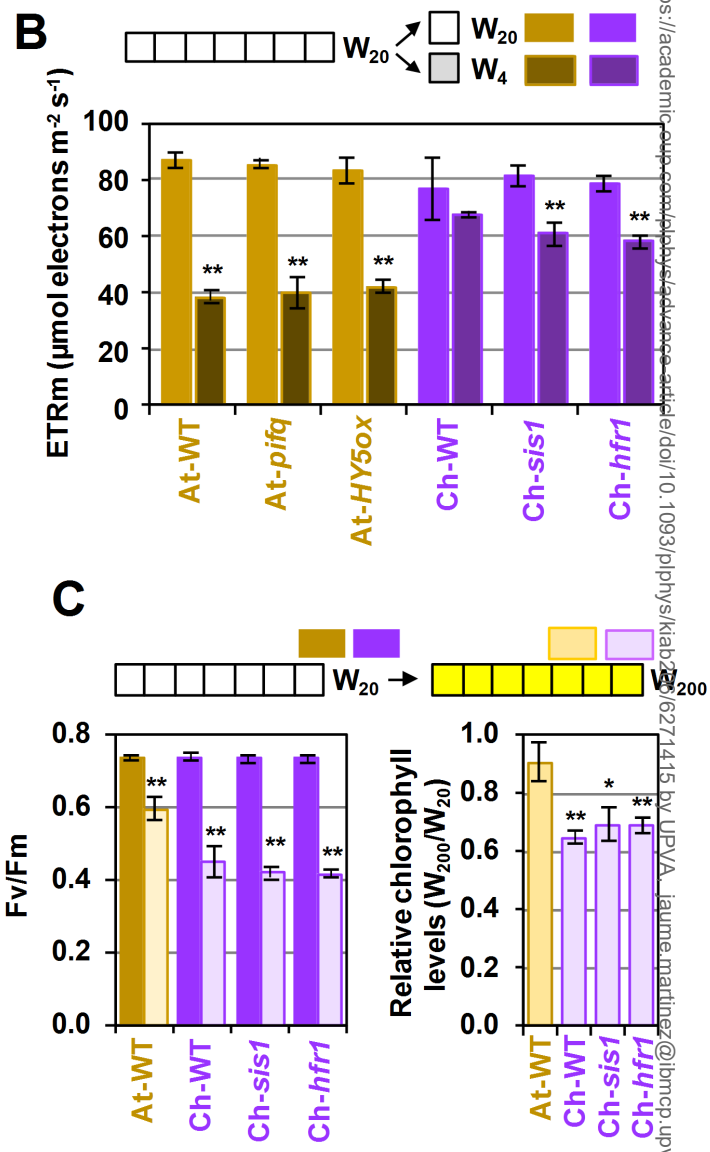
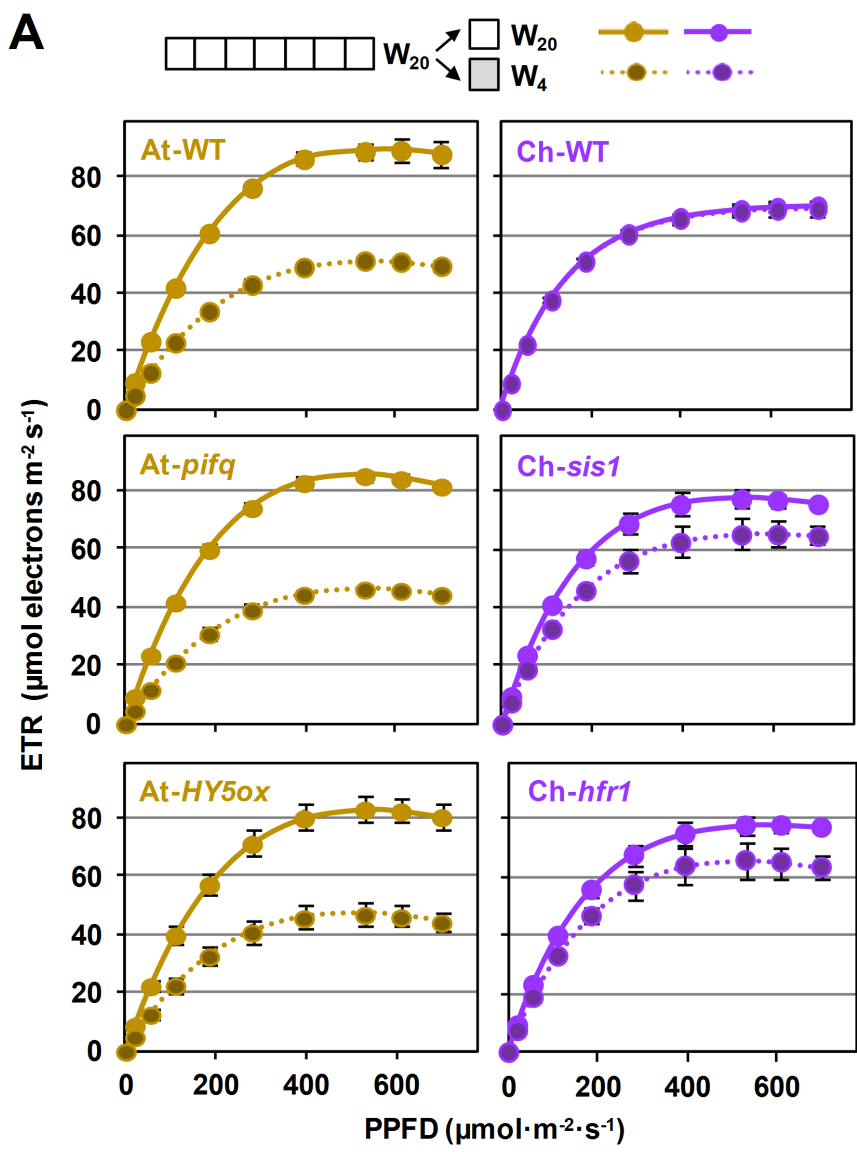


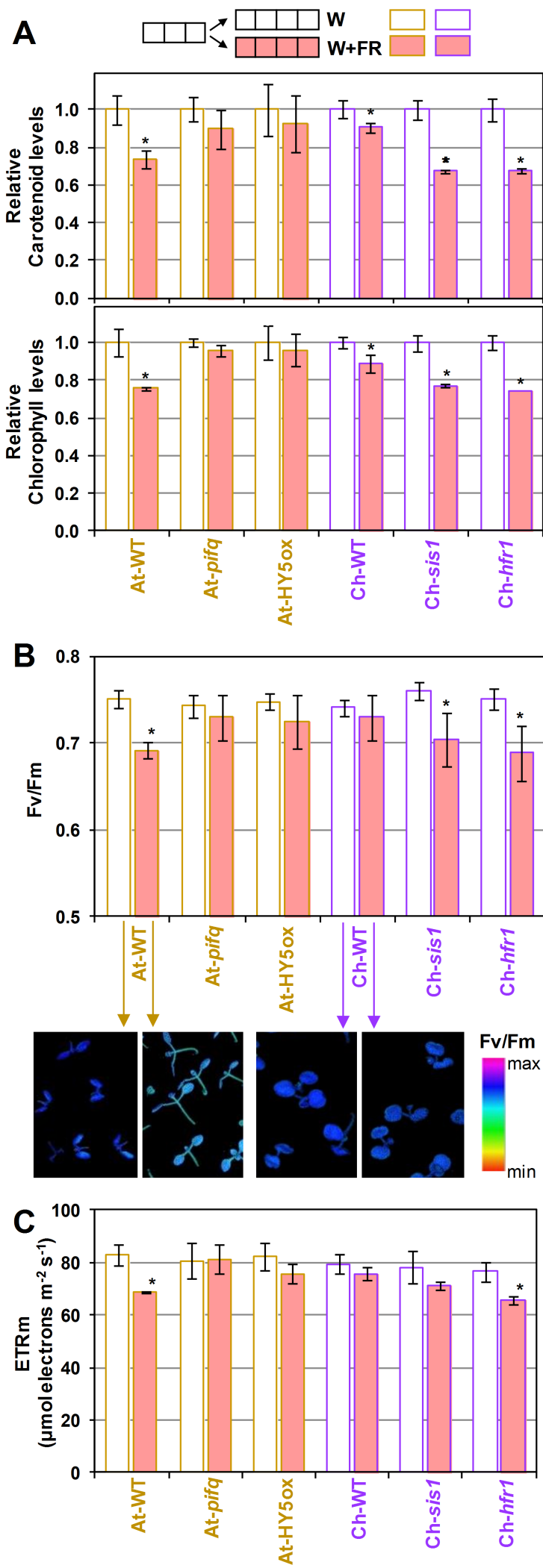
A

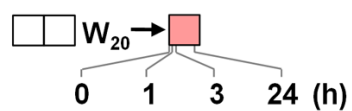


B





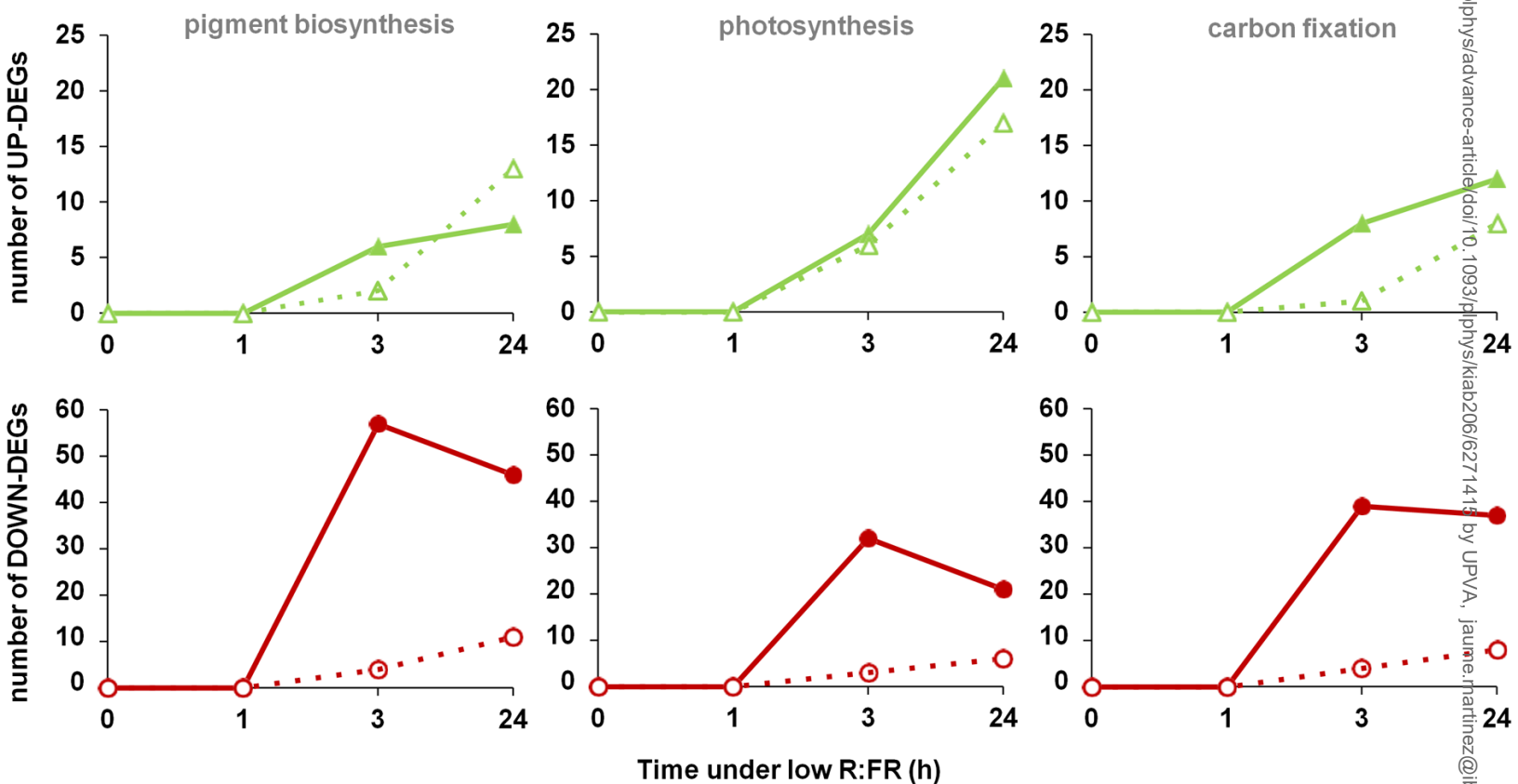


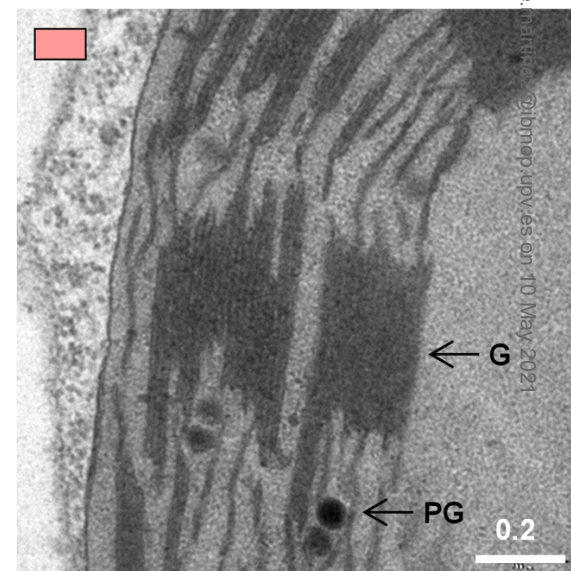
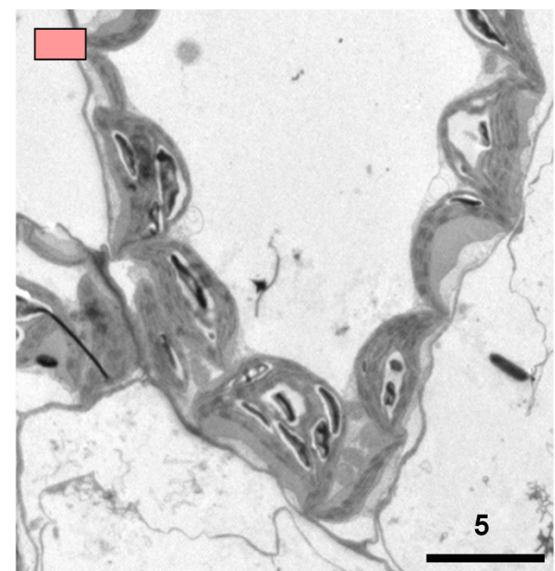
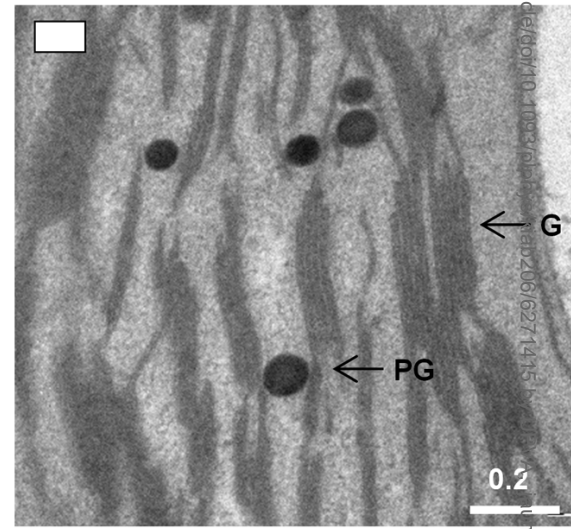
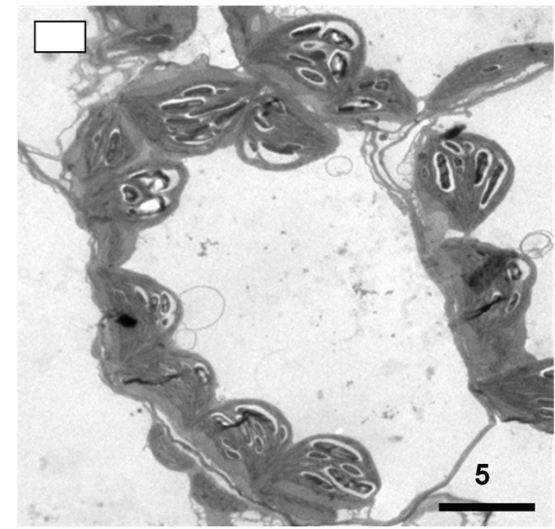
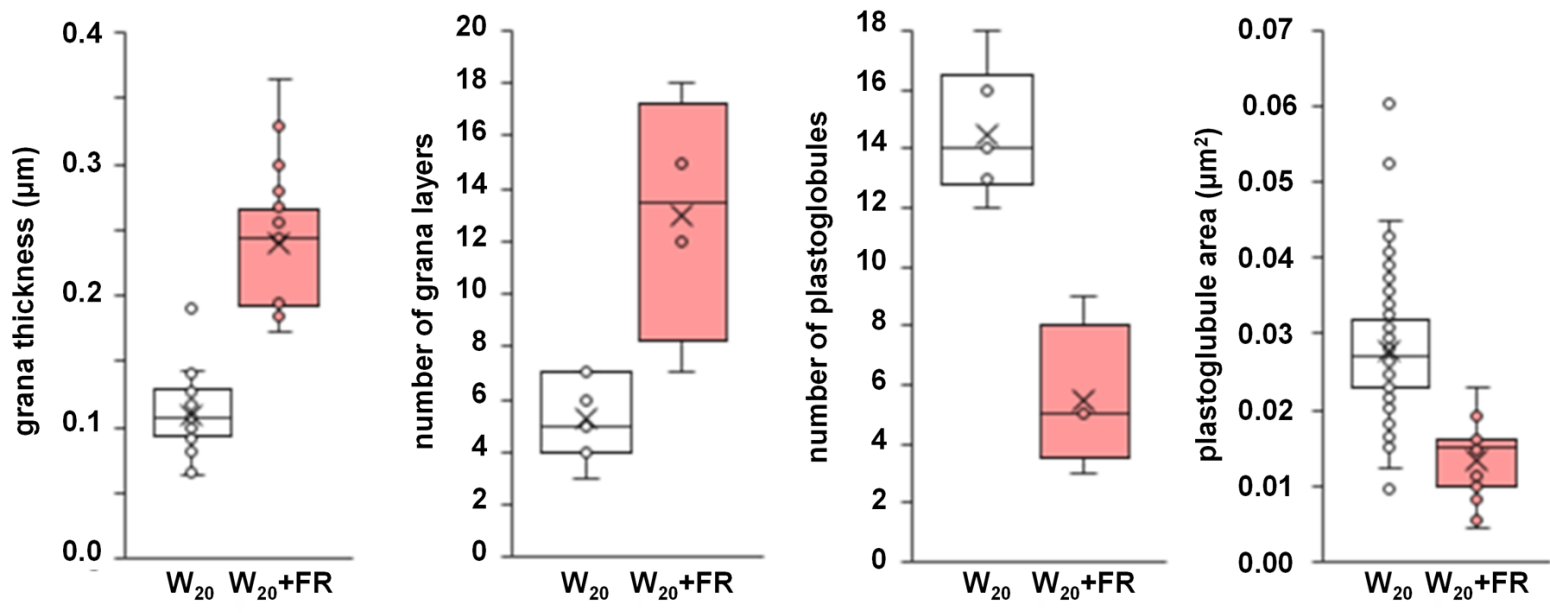
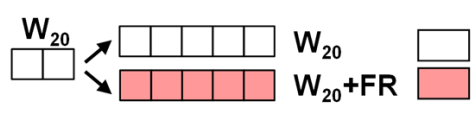


UP-regulated in $W_{20}+FR$ vs. W_{20}

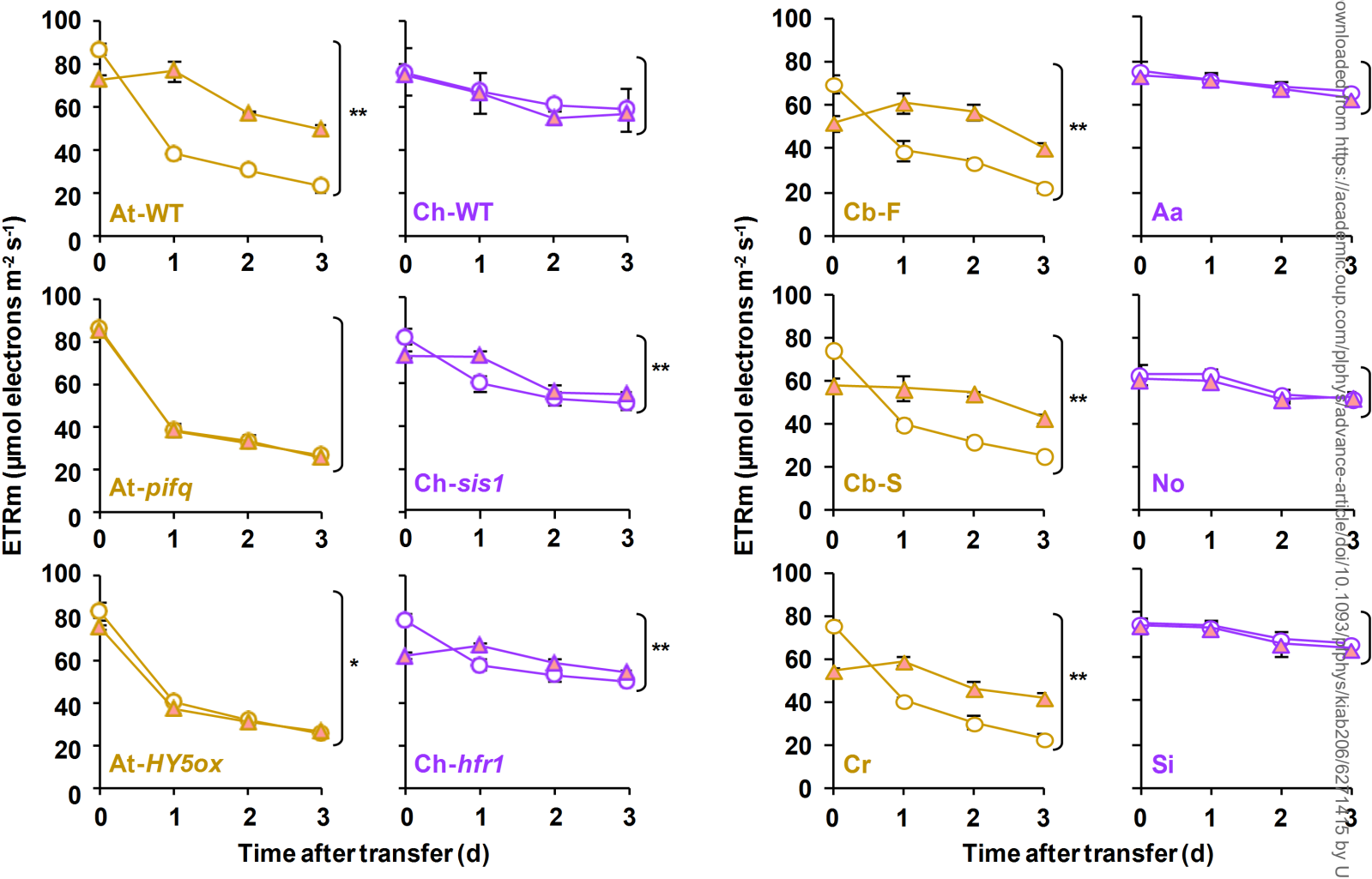
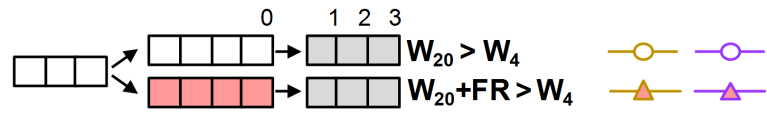
DOWN-regulated in $W_{20}+FR$ vs. W_{20}

▲ *At-WT* ▲ *At-pifq*
● *At-WT* ● *At-pifq*

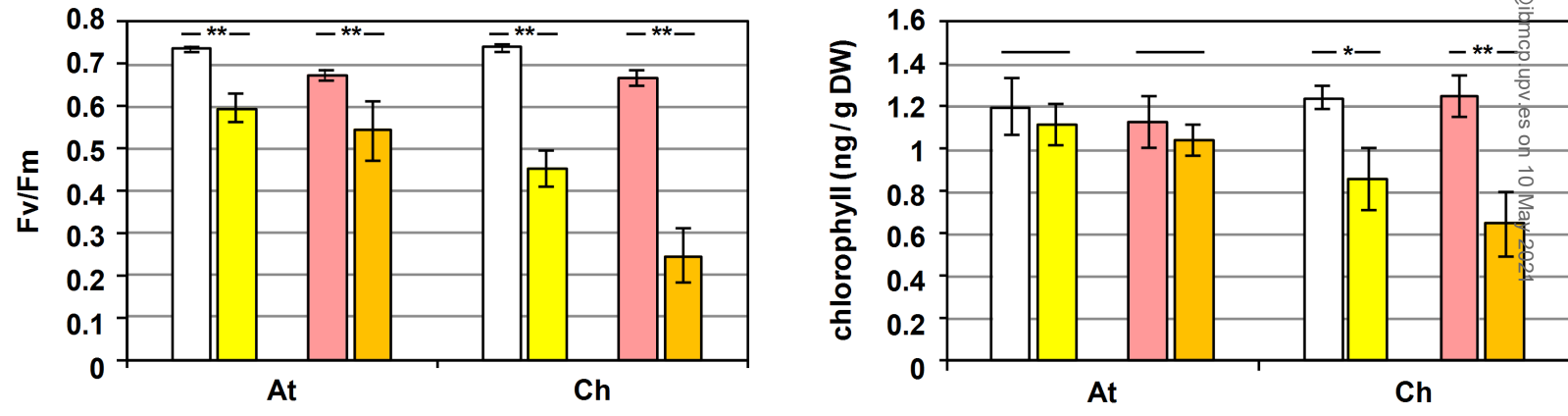
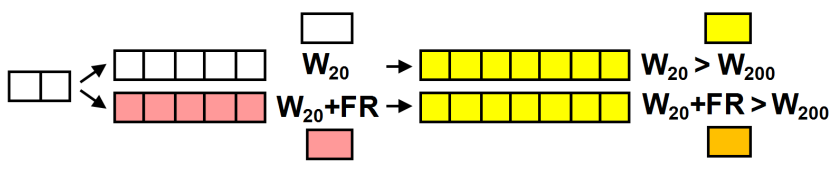




A



B



Parsed Citations

- Bailey S, Walters RG, Jansson S, Horton P (2001) Acclimation of *Arabidopsis thaliana* to the light environment: the existence of separate low light and high light responses. *Planta* 213: 794-801
Google Scholar: [Author Only](#) [Title Only](#) [Author and Title](#)
- Benkov MA, Yatsenko AM, Tikhonov AN (2019) Light acclimation of shade-tolerant and sun-resistant *Tradescantia* species: photochemical activity of PSII and its sensitivity to heat treatment. *Photosynth Res* 139: 203-214
Google Scholar: [Author Only](#) [Title Only](#) [Author and Title](#)
- Bou-Torrent J, Toledo-Ortiz G, Ortiz-Alcaide M, Cifuentes-Esquivel N, Halliday KJ, Martinez-Garcia JF, Rodriguez-Concepcion M (2015) Regulation of Carotenoid Biosynthesis by Shade Relies on Specific Subsets of Antagonistic Transcription Factors and Cofactors. *Plant Physiol* 169: 1584-1594
Google Scholar: [Author Only](#) [Title Only](#) [Author and Title](#)
- Cagnola JI, Ploschuk E, Benech-Arnold T, Finlayson SA, Casal JJ (2012) Stem transcriptome reveals mechanisms to reduce the energetic cost of shade-avoidance responses in tomato. *Plant Physiol* 160: 1110-1119
Google Scholar: [Author Only](#) [Title Only](#) [Author and Title](#)
- Casal JJ (2013) Photoreceptor signaling networks in plant responses to shade. *Annu Rev Plant Biol* 64: 403-427
Google Scholar: [Author Only](#) [Title Only](#) [Author and Title](#)
- Cifuentes-Esquivel N, Bou-Torrent J, Galstyan A, Galleni M, Sessa G, Salla Martret M, Roig-Villanova I, Ruberti I, Martinez-Garcia JF (2013) The bHLH proteins BEE and BIM positively modulate the shade avoidance syndrome in *Arabidopsis* seedlings. *The Plant Journal* 75: 989-1002
Google Scholar: [Author Only](#) [Title Only](#) [Author and Title](#)
- Cioffi A, Sessa G, Sassi M, Possenti M, Salvucci S, Carabelli M, Morelli G, Ruberti I (2013) Dynamics of the shade-avoidance response in *Arabidopsis*. *Plant Physiol* 163: 331-353
Google Scholar: [Author Only](#) [Title Only](#) [Author and Title](#)
- de Wit M, Ljung K, Fankhauser C (2015) Contrasting growth responses in lamina and petiole during neighbor detection depend on differential auxin responsiveness rather than different auxin levels. *New Phytol* 208: 198-209
Google Scholar: [Author Only](#) [Title Only](#) [Author and Title](#)
- Flores-Perez U, Sauret-Gueto S, Gas E, Jarvis P, Rodriguez-Concepcion M (2008) A mutant impaired in the production of plastome-encoded proteins uncovers a mechanism for the homeostasis of isoprenoid biosynthetic enzymes in *Arabidopsis* plastids. *Plant Cell* 20: 1303-1315
Google Scholar: [Author Only](#) [Title Only](#) [Author and Title](#)
- Florez-Sarasa I, Ostaszewska M, Galle A, Flexas J, Rychter AM, Ribas-Carbo M (2009) Changes of alternative oxidase activity, capacity and protein content in leaves of *Cucumis sativus* wild-type and MSC16 mutant grown under different light intensities. *Physiol Plant* 137: 419-426
Google Scholar: [Author Only](#) [Title Only](#) [Author and Title](#)
- Galstyan A, Cifuentes-Esquivel N, Bou-Torrent J, Martinez-Garcia JF (2011) The shade avoidance syndrome in *Arabidopsis*: a fundamental role for atypical basic helix-loop-helix proteins as transcriptional cofactors. *Plant J* 66: 258-267
Google Scholar: [Author Only](#) [Title Only](#) [Author and Title](#)
- Galleni M, Molina-Contreras MJ, Paulisic S, Salla-Martret M, Sorin C, Godoy M, Franco-Zorrilla JM, Solano R, Martinez-Garcia JF (2017) A non-DNA-binding activity for the ATHB4 transcription factor in the control of vegetation proximity. *New Phytol* 216: 798-813
Google Scholar: [Author Only](#) [Title Only](#) [Author and Title](#)
- Hay AS, Pieper B, Cooke E, Mandakova T, Cartolano M, Tattersall AD, Ioio RD, McGowan SJ, Barkoulas M, Galinha C et al (2014) *Cardamine hirsuta*: a versatile genetic system for comparative studies. *Plant J* 78: 1-15
Google Scholar: [Author Only](#) [Title Only](#) [Author and Title](#)
- Hornitschek P, Lorrain S, Zoete V, Michielin O, Fankhauser C (2009) Inhibition of the shade avoidance response by formation of non-DNA binding bHLH heterodimers. *EMBO J* 28: 3893-3902
Google Scholar: [Author Only](#) [Title Only](#) [Author and Title](#)
- Igamberdiev AU, Eprintsev AT, Fedorin DN, Popov VN (2014) Phytochrome-mediated regulation of plant respiration and photorespiration. *Plant Cell Environ* 37: 290-299
Google Scholar: [Author Only](#) [Title Only](#) [Author and Title](#)
- Kanehisa M, Sato Y (2020) KEGG Mapper for inferring cellular functions from protein sequences. *Protein Sci* 29: 28-35
Google Scholar: [Author Only](#) [Title Only](#) [Author and Title](#)
- Koenig D, Hagmann J, Li R, Bemm F, Slotte T, Neuffer B, Wright SI, Weigel D (2019) Long-term balancing selection drives evolution of immunity genes in *Capsella*. *Elife* 8
Google Scholar: [Author Only](#) [Title Only](#) [Author and Title](#)
- Kohnen MV, Schmid-Siegert E, Trevisan M, Petrolati LA, Senechal F, Muller-Moule P, Maloof J, Xenarios I, Fankhauser C (2016)

Neighbor Detection Induces Organ-Specific Transcriptomes, Revealing Patterns Underlying Hypocotyl-Specific Growth. *Plant Cell* 28: 2889-2904

Google Scholar: [Author Only](#) [Title Only](#) [Author and Title](#)

Leivar P, Tepperman JM, Cohn MM, Monte E, Al-Sady B, Erickson E, Quail PH (2012) Dynamic antagonism between phytochromes and PIF family basic helix-loop-helix factors induces selective reciprocal responses to light and shade in a rapidly responsive transcriptional network in Arabidopsis. *Plant Cell* 24: 1398-1419

Google Scholar: [Author Only](#) [Title Only](#) [Author and Title](#)

Lichtenthaler HK (2007) Biosynthesis, accumulation and emission of carotenoids, alpha-tocopherol, plastoquinone, and isoprene in leaves under high photosynthetic irradiance. *Photosynth Res* 92: 163-179

Google Scholar: [Author Only](#) [Title Only](#) [Author and Title](#)

Lorenzo CD, Alonso Iserte J, Sanchez Lamas M, Antonietti MS, Garcia Gagliardi P, Hernando CE, Dezar CAA, Vazquez M, Casal JJ, Yanovsky MJ et al (2019) Shade delays flowering in *Medicago sativa*. *Plant J* 99: 7-22

Google Scholar: [Author Only](#) [Title Only](#) [Author and Title](#)

Martin G, Leivar P, Ludevid D, Tepperman JM, Quail PH, Monte E (2016) Phytochrome and retrograde signalling pathways converge to antagonistically regulate a light-induced transcriptional network. *Nat Commun* 7: 11431

Google Scholar: [Author Only](#) [Title Only](#) [Author and Title](#)

Martinez-Garcia JF, Galstyan A, Salla-Martret M, Cifuentes-Esquivel N, Gallemí M, Bou-Torrent J (2010) Regulatory components of shade avoidance syndrome. *Advances in Botanical Research* 53: 65-116

Google Scholar: [Author Only](#) [Title Only](#) [Author and Title](#)

Martinez-Garcia JF, Gallemí M, Molina-Contreras MJ, Llorente B, Bevilacqua MR, Quail PH (2014) The shade avoidance syndrome in *Arabidopsis*: the antagonistic role of phytochrome a and B differentiates vegetation proximity and canopy shade. *PLoS One* 9: e109275

Google Scholar: [Author Only](#) [Title Only](#) [Author and Title](#)

Molina-Contreras MJ, Paulisic S, Then C, Moreno-Romero J, Pastor-Andreu P, Morelli L, Roig-Villanova I, Jenkins H, Hallab A, Gan X et al (2019) Photoreceptor Activity Contributes to Contrasting Responses to Shade in Cardamine and Arabidopsis Seedlings. *Plant Cell* 31: 2649-2663

Google Scholar: [Author Only](#) [Title Only](#) [Author and Title](#)

Murchie EH, Horton P (1997) Acclimation of photosynthesis to irradiance and spectral quality in British plant species: chlorophyll content, photosynthetic capacity and habitat preference *Plant Cell Environ* 20: 438-448

Google Scholar: [Author Only](#) [Title Only](#) [Author and Title](#)

Ortiz-Alcaide M, Llamas E, Gomez-Cadenas A, Nagatani A, Martinez-Garcia JF, Rodriguez-Concepcion M (2019) Chloroplasts modulate elongation responses to canopy shade by retrograde pathways involving HY5 and ABA *Plant Cell*

Google Scholar: [Author Only](#) [Title Only](#) [Author and Title](#)

Patel D, Basu M, Hayes S, Majlath I, Hetherington FM, Tschaplinski TJ, Franklin KA (2013) Temperature-dependent shade avoidance involves the receptor-like kinase ERECTA *Plant J* 73: 980-992

Google Scholar: [Author Only](#) [Title Only](#) [Author and Title](#)

Paulisic S, Qin W, Arora Veraszto H, Then C, Alary B, Nogue F, Tsiantis M, Hothorn M, Martinez-Garcia JF (2021) Adjustment of the PIF7-HFR1 transcriptional module activity controls plant shade adaptation. *EMBO J* 40: e104273

Google Scholar: [Author Only](#) [Title Only](#) [Author and Title](#)

Platt T, Gallegos CL, Harrison WG (1980) Photoinhibition of photosynthesis in natural assemblages of marine phytoplankton. *Journal of Marine Research* 38: 687-701

Google Scholar: [Author Only](#) [Title Only](#) [Author and Title](#)

Pons TL, Poorter H (2014) The effect of irradiance on the carbon balance and tissue characteristics of five herbaceous species differing in shade-tolerance. *Front Plant Sci* 5: 12

Google Scholar: [Author Only](#) [Title Only](#) [Author and Title](#)

Ptushenko OS, Ptushenko VV (2019) Tradescantia-based models: a powerful looking glass for investigation of photoacclimation and photoadaptation in plants. *Physiol Plant* 166: 120-133

Google Scholar: [Author Only](#) [Title Only](#) [Author and Title](#)

Ribas-Carbo M, Giles L, Flexas J, Briggs W, Berry JA (2008) Phytochrome-driven changes in respiratory electron transport partitioning in soybean (*Glycine max. L.*) cotyledons. *Plant Biol (Stuttg)* 10: 281-287

Google Scholar: [Author Only](#) [Title Only](#) [Author and Title](#)

Roig-Villanova I, Bou-Torrent J, Galstyan A, Carretero-Paulet L, Portoles S, Rodriguez-Concepcion M, Martinez-Garcia JF (2007) Interaction of shade avoidance and auxin responses: a role for two novel atypical bHLH proteins. *The EMBO Journal* 26: 4756-4767

Google Scholar: [Author Only](#) [Title Only](#) [Author and Title](#)

Roig-Villanova I, Martinez-Garcia JF (2016) Plant Responses to Vegetation Proximity: A Whole Life Avoiding Shade. *Front Plant Sci* 7: 236

Google Scholar: [Author Only](#) [Title Only](#) [Author and Title](#)

- Roig-Villanova I, Paulisic S, Martinez-Garcia JF (2019) Shade Avoidance and Neighbor Detection. *Methods Mol Biol* 2026: 157-168**
Google Scholar: [Author Only](#) [Title Only](#) [Author and Title](#)
- Rozak PR, Seiser RM, Wacholtz WF, Wise RR (2002) Rapid, reversible alterations in spinach thylakoid appression upon changes in light intensity. *Plant Cell Environ* 25: 421-429**
Google Scholar: [Author Only](#) [Title Only](#) [Author and Title](#)
- Ruckle ME, DeMarco SM, Larkin RM (2007) Plastid signals remodel light signaling networks and are essential for efficient chloroplast biogenesis in *Arabidopsis*. *Plant Cell* 19: 3944-3960**
Google Scholar: [Author Only](#) [Title Only](#) [Author and Title](#)
- Schindelin J, Arganda-Carreras I, Frise E, Kaynig V, Longair M, Pietzsch T, Preibisch S, Rueden C, Saalfeld S, Schmid B et al (2012) Fiji: an open-source platform for biological-image analysis. *Nat Methods* 9: 676-682**
Google Scholar: [Author Only](#) [Title Only](#) [Author and Title](#)
- Shi Q, Kong F, Zhang H, Jiang Y, Heng S, Liang R, Ma L, Liu J, Lu X, Li P et al (2019) Molecular mechanisms governing shade responses in maize. *Biochem Biophys Res Commun* 516: 112-119**
Google Scholar: [Author Only](#) [Title Only](#) [Author and Title](#)
- Smith H (1982) Light quality, photoperception, and plant strategy. *Annual Review of Plant Physiology* 33: 481-518**
Google Scholar: [Author Only](#) [Title Only](#) [Author and Title](#)
- Sterck FJ, Duurssma RA, Pearcy RW, Valladares F, Cieslak M, Weemstra M (2013) Plasticity influencing the light compensation point offsets the specialization for light niches across shrub species in a tropical forest understorey. *Journal of Ecology* 101: 971-980**
Google Scholar: [Author Only](#) [Title Only](#) [Author and Title](#)
- Toledo-Ortiz G, Johansson H, Lee KP, Bou-Torrent J, Stewart K, Steel G, Rodriguez-Concepcion M, Halliday KJ (2014) The HY5-PIF regulatory module coordinates light and temperature control of photosynthetic gene transcription. *PLoS Genet* 10: e1004416**
Google Scholar: [Author Only](#) [Title Only](#) [Author and Title](#)
- Valladares F, Niinemets U (2008) Shade Tolerance, a Key Plant Feature of Complex Nature and Consequences. *Annual Review of Ecology, Evolution, and Systematics* 39: 237-257**
Google Scholar: [Author Only](#) [Title Only](#) [Author and Title](#)
- Wang R, Farrona S, Vincent C, Joecker A, Schoof H, Turck F, Alonso-Blanco C, Coupland G, Albani MC (2009) PEP1 regulates perennial flowering in *Arabidopsis*. *Nature* 459: 423-427**
Google Scholar: [Author Only](#) [Title Only](#) [Author and Title](#)
- Wood WHJ, MacGregor-Chatwin C, Barnett SFH, Mayneord GE, Huang X, Hobbs JK, Hunter CN, Johnson MP (2018) Dynamic thylakoid stacking regulates the balance between linear and cyclic photosynthetic electron transfer. *Nat Plants* 4: 116-127**
Google Scholar: [Author Only](#) [Title Only](#) [Author and Title](#)
- Xu X, Chi W, Sun X, Feng P, Guo H, Li J, Lin R, Lu C, Wang H, Leister D et al (2016) Convergence of light and chloroplast signals for de-etiolation through ABI4-HY5 and COP1. *Nat Plants* 2: 16066**
Google Scholar: [Author Only](#) [Title Only](#) [Author and Title](#)
- Yang C, Xie F, Jiang Y, Li Z, Huang X, Li L (2018) Phytochrome A Negatively Regulates the Shade Avoidance Response by Increasing Auxin/Indole Acetic Acid Protein Stability. *Dev Cell* 44: 29-41 e24**
Google Scholar: [Author Only](#) [Title Only](#) [Author and Title](#)